Lawrence Berkeley National Laboratory
LBL Publications

Title
From Design to Device: Challenges and Opportunities in Computational Discovery of p-Type Transparent Conductors

Permalink
https://escholarship.org/uc/item/2397w0g2

Journal
PRX Energy, 3(3)

ISSN
2768-5608

Authors
Woods-Robinson, Rachel
Morales-Masis, Monica
Hautier, Geoffroy
et al.

Publication Date
2024-08-01

DOI
10.1103/prxenergy.3.031001

Copyright Information
This work is made available under the terms of a Creative Commons Attribution License, available at https://creativecommons.org/licenses/by/4.0/

Peer reviewed

eScholarship.org Powered by the California Digital Library
University of California

Perspective

From Design to Device: Challenges and Opportunities in Computational Discovery of *p*-Type Transparent Conductors

Rachel Woods-Robinson,[1,2,3,*] Monica Morales-Masis,[4] Geoffroy Hautier,[5] and Andrea Crovetto[6]

[1] *Clean Energy Institute, University of Washington, Seattle, Washington 98195, USA*
[2] *Materials Sciences Division, Lawrence Berkeley National Laboratory, Berkeley, California 94720, USA*
[3] *Materials Science Center, National Renewable Energy Laboratory, Golden, Colorado 80401, USA*
[4] *MESA+ Institute for Nanotechnology, University of Twente, Enschede 7500 AE, Netherlands*
[5] *Thayer School of Engineering, Dartmouth College, 14 Engineering Dr, Hanover, New Hampshire, 03755, USA*
[6] *Centre for Nano Fabrication and Characterization (DTU Nanolab), Technical University of Denmark, Kongens Lyngby, 2800, Denmark*

(Received 29 January 2024; revised 17 May 2024; published 5 August 2024)

A high-performance *p*-type transparent conductor (TC) does not yet exist but could lead to advances in a wide range of optoelectronic applications and enable new architectures for, e.g., next-generation photovoltaic (PV) devices. High-throughput computational material screenings have been a promising approach to filter databases and identify new *p*-type TC candidates and some of these predictions have been experimentally validated. However, most of these predicted candidates do not have experimentally achieved properties on par with *n*-type TCs used in solar cells and therefore have not yet been used in commercial devices. Thus, there is still a significant divide between transforming predictions into results that are actually achievable in the laboratory and an even greater lag in scaling predicted materials into functional devices. In this perspective, we outline some of the major disconnects in this materials discovery process—from scaling computational predictions into synthesizable crystals and thin films in the laboratory to scaling laboratory-grown films into real-world solar devices—and share insights to inform future strategies for TC discovery and design.

DOI: 10.1103/PRXEnergy.3.031001

I. INTRODUCTION

Many advances in renewable energy technology are limited by the quality and availability of materials. Conversely, materials advances enable technological advances. The search for *p*-type transparent conductors (TCs) exemplify this: achieving a *p*-type TC with comparable properties to *n*-type transparent conducting oxides (TCOs) could enable architectures and applications for solar cells and transparent electronics, serving as hole-selective top contacts or electrodes, buffer layers, back contacts for bifacial solar cells, and window layers in tandem devices [1,2]. Many candidate *p*-type TCs have been proposed and explored, such as delafossites CuMO$_2$ [3] and CuI [4], among others. Yet the realization of high-performing *p*-type TCs is still a major research challenge and *p*-type TCs for photovoltaic (PV) applications remain limited. This is in part due to fundamental physical trade-offs of combining transparency, *p*-type doping, and high hole mobilities in wide-band-gap oxides [5].

While the first *p*-type TCs have been found by serendipity and following chemical principles (e.g., Cu-based TCs), it is now possible to identify new *p*-type TCs using first-principles computations and high-throughput screening. "High-throughput" computational screenings usually begin with selection of a set of input compounds often from material databases (e.g., Materials Project [6], AFLOW [7], and OQMD [8], among others), followed by a series of filtration steps using computed descriptors that represent proxies for certain materials properties [9].

As depicted in Fig. 1(a), after selection of inputs, a typical screening method for *p*-type TCs starts with (1) a proxy for thermodynamic stability (usually energy above convex hull, E_{hull}), (2) a proxy for the absorption edge above the visible regime (usually the Kohn-Sham band

*Contact author: rwoodsr@uw.edu

Published by the American Physical Society under the terms of the Creative Commons Attribution 4.0 International license. Further distribution of this work must maintain attribution to the author(s) and the published article's title, journal citation, and DOI. Open access publication funded by National Renewable Energy Laboratory (NREL) Library, part of a national laboratory of the U.S. Department of Energy.

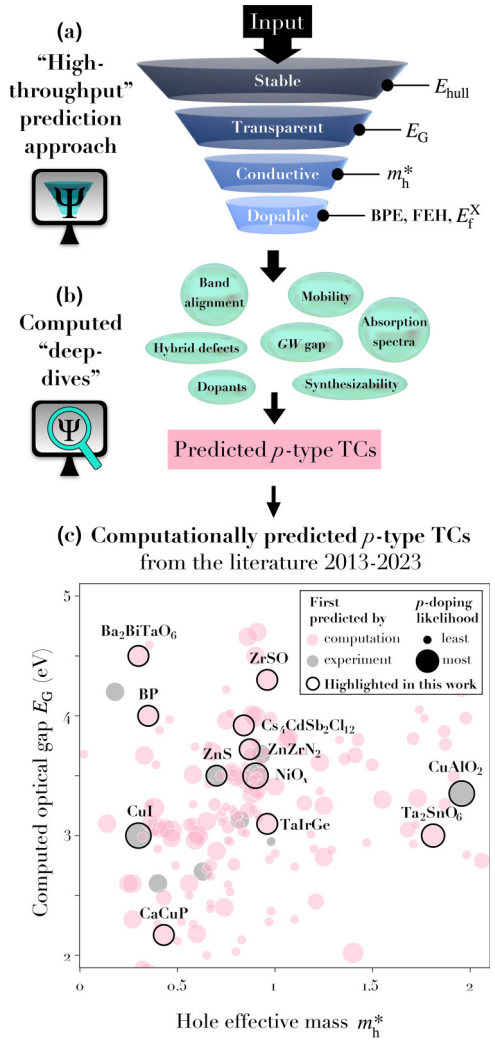

FIG. 1. (a) An example of a high-throughput screening method for p-type TCs [12]. (b) An example of properties that are assessed during "deep-dive" calculations. (c) A 2013–2023 literature review of p-type TC candidates predicted from high-throughput computational studies, with candidates highlighted that are discussed in this paper. Pink-shaded materials have been predicted first as p-type TCs by computation, while gray-shaded materials have been first demonstrated experimentally and are included here as references. "Most" likely p-type dopable materials have been confirmed by experiment or have hybrid defect calculations, while "least" likely have not been assessed for dopability. A comprehensive table with references of computational studies of p-type TCs and a JUPYTER notebook to reproduce (c) are provided in the Supplemental Material [34].

gap, E_G), and (3) a proxy for high hole mobility (usually hole effective mass, m_h^*), followed by a series of more computationally demanding calculations for hole dopability, band alignment, synthesizability, and other properties [10–13]. As final screening steps, as shown in Fig. 1(b), higher-accuracy computational methods can be applied, such as hybrid or GW computations (to better estimate transparency) or electron-phonon limited mobility (to estimate hole transport).

Computational screening research from the past decade has yielded promising p-type TC candidates and key discoveries are summarized in Fig. 1. One of the earliest studies focused on oxides and identified a handful of new p-type TCO candidates [10]. Since then, a wide array of follow-up research has refined the screening criteria or input material set; e.g., by extending the chemistries of interest beyond ternary oxides or by focusing on specific chemistries or structures [11,14–24]. These studies have motivated the synthesis and characterization of a handful of computationally identified candidates, with a few notable success stories. For example, very high mobility and transparency have been observed experimentally in moderately p-type Ba_2BiTaO_6 [15,25] and TaIrGe [26]. Transparency and high p-type dopability has been confirmed experimentally in Cr_2MnO_4, although with lower hole mobilities [14]. Overviews of experimentally realized p-type TCs can be found in existing literature reviews and benchmarking studies [2]. These successes, some of which are highlighted in Fig. 5, are encouraging and bring a new level of predictability for computational materials science.

However, the experimental confirmation of certain predictions has been either incomplete or not up to the expectations of the prediction. Boron phosphide (BP), for instance, has been identified as a promising p-type TC with previous encouraging experimental results but recent results indicate a difficulty to reach expected performances, as described later in this paper [11,27,28]. Ta_2SnO_6 showed promise and yet could not be doped enough to measure hole conductivity [29]. Other predicted materials remain to be grown and evaluated, ideally in thin-film form (e.g., $K_2Sn_2O_3$, B_6O, $NaNbO_2$, and $BeSiP_2$) [10,22,30]. Progress in the field of predicted n-type TCs serves as an indicator that advances in predicted p-type TCs are within reach; e.g., as a success of a high-throughput screening, a new computationally predicted n-type TCO $ZnSb_2O_6$ has been recently confirmed by experiment with high doping and mobility [31,32]. However, despite the many successes, scaling up predicted TCs for efficient optoelectronic device applications remains a major challenge, and a variety of disconnects have emerged.

Historically, unwanted laboratory results and corresponding insights from researchers are usually not published, leading to a literature bias and a difficulty disentangling why disconnects are occurring. In this paper, we identify and contextualize these disconnects observed in the literature and within our own research in scaling p-type TC predictions into PV devices. First, we design a framework for the different stages involved in this process, as summarized in Fig. 3. Next, we highlight some of the most pernicious disconnects (see Fig. 4). One set of disconnects stem from transforming predicted candidates into

thin films in the laboratory: due to challenges including synthesizability, phase purity, dopability, and unwanted absorption, so far no predicted p-type TC grown in the laboratory performs on par with n-type TCOs. Another key set of disconnect arises from transforming predictions into scalable optoelectronic devices: challenges emerge, such as making sufficient contact to the device, tuning band alignments, and growing interfaces free of defects and other barriers. We also discuss specific barriers related to scalability and sustainability. Lastly, we offer guidance on how the research community can overcome such disconnects to bring our predictions into fruition in p-TCs and beyond.

II. MATERIALS DESIGN-TO-DEVICE FRAMEWORK FOR p-TYPE TCs

A. PV applications of p-type TCs

While conventional silicon (Si) solar modules do not typically include contact layers, emerging PV technologies such as silicon heterojunction (SHJ), tunnel-oxide passivated contact (TOPCon), thin film (e.g., CdTe, perovskites, and other direct-band-gap absorbers), and tandem solar cells require various contact- and buffer-layer configurations to transfer charge carriers throughout the device. The current market share of PV (as of 2024) is mostly conventional Si, however various projections show that meeting our net-zero requirements by 2050 will likely require rapid development and scaling of such emerging PV technology [33].

One recent study projects deployment of these emerging PV technologies to ramp up rapidly after 2030 and by around 2040 overtake conventional silicon as the dominant PV technology [35]. However, as researchers develop these new configurations, few options for inorganic p-type transparent contacts (which generally have better conductivity and stability than organic hole-transport materials) are available and this limits available architectures and resulting performance. Therefore, developing appropriate contact materials for emerging PV applications, especially p-type transparent contacts, is an important research direction.

Applications for p-type TCs span far beyond solar (e.g., flat panel displays, transparent electronics, etc.) but for the purposes of this paper we focus mainly on PV devices. Within the field of emerging PV applications, p-type TCs with different properties could serve a variety of roles. For example, p-type TCs could have a double role, that of a hole-conducting carrier-selective contact (where a high work function is required) and that of a transparent electrode (where a low sheet resistance is required, usually below 100 Ω/sq). As a selective contact, the p-type TC would extract photogenerated holes in the absorber material and, as a transparent electrode, it would laterally transport the carriers to the device terminal. Since the material is transparent, it would also function as a window layer in the device. This would enable novel device architectures for, e.g., bifacial and semitransparent PV devices, which currently relies exclusively on the use of n-type ITO.

Representative device designs are summarized in Fig. 2, with future applications enabled by high-performance p-type TCs highlighted in yellow in Figs. 2(a)– 2(c). Designing TCs with high lateral (or "in-plane") transport for these applications will be the focus of this paper. For reference, we also show two "out-of-plane" transport configurations [Figs. 2(d) and 2(e)] in which mobility and dopability are less important, buffer HTLs, and semitransparent contacts (in which transparency is less important); since these applications have actually been demonstrated, they will be used to showcase challenges scaling to devices in Sec. IV but are not the focus of this paper. This variety of applications is the origin of one important disconnect, which arises from an intermingling of problem statements during the materials design stage. Namely, a material predicted from an application-agnostic screening for p-type TCs may not be appropriate to use in a specific application, e.g., might not provide an adequate band alignment.

B. Materials discovery stages

To understand the disconnects that emerge when scaling up computationally predicted materials, we first summarize the main stages involved in going from a predicted material, to a synthesized material, to the exploration of its functionality on a device, and to a commercially relevant device. For the specific case of a p-type transparent conductor (p-type TC), the "design-to-device" framework is summarized in Fig. 3, with the following nine key stages:

(1) *Computational screening*. As shown in Fig. 1(a), a material is "screened" as a promising candidate, often from a database. Simple computational metrics representing properties of stability, transparency, and conductivity are evaluated. Usually, a stoichiometric well-defined crystal structure is assumed, though high-throughput defects have started to emerge and could be used at this stage [36,37]. Various biases can occur at this early stage that introduce disconnects at later stages.

(2) *Computational deep dive*. Higher levels of theory (e.g., spin-orbit coupling and *GW*) and more in-depth analysis methods are applied to more accurately predict properties of synthesizability, transparency, temperature-dependent mobility, carrier concentration from defects, and device-relevant parameters such as band alignment, as shown in Fig. 1(b). Structural models can be more complex at this stage to account for off-stoichiometric and nonequilibrium effects.

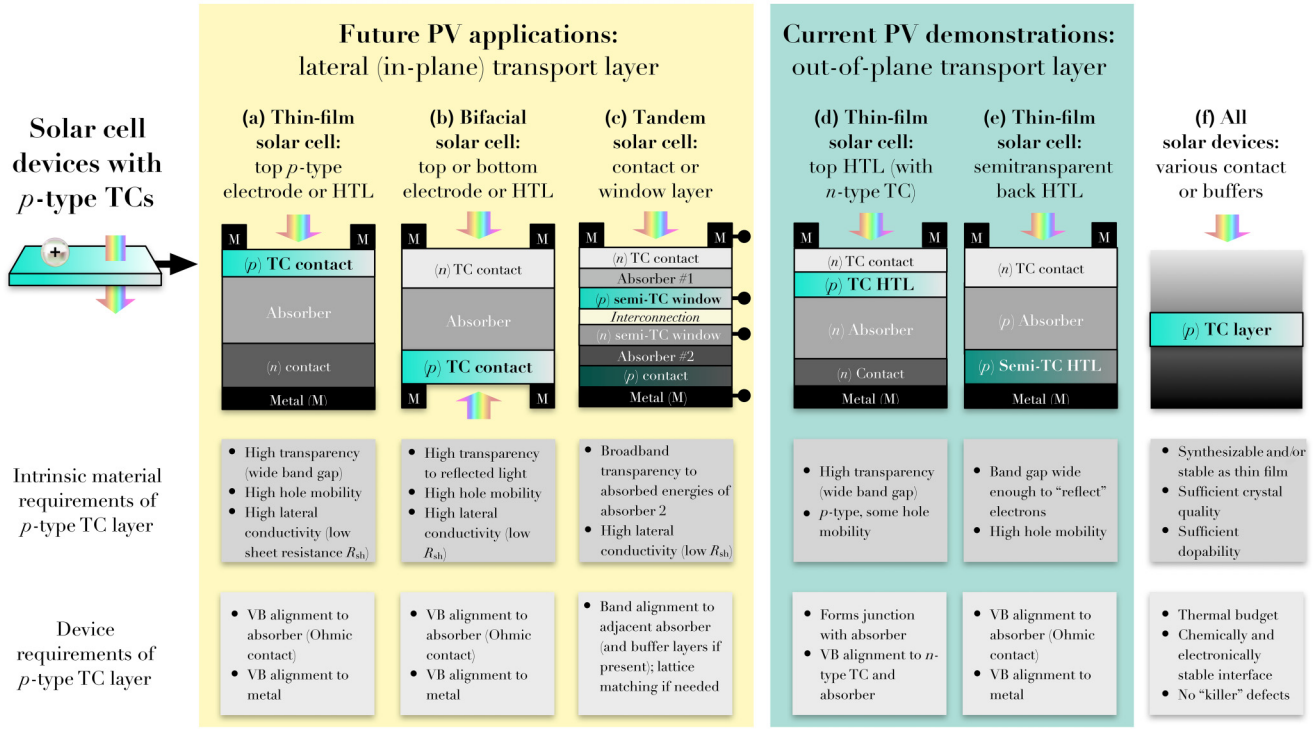

FIG. 2. Schematics of solar cell device architectures that incorporate p-type TCs. The intent behind the materials highlighted in this paper is to enable architectures for "Future PV applications," including as (a) a top p-type electrode to a thin-film single junction stack, (b) a top or bottom electrode to a bifacial solar cell, and (c) as a contact or window layer to a tandem solar cell. Panel (c) depicts a four-terminal (4T) mechanically stacked tandem, in which a p-type semitransparent conductor ("semi-TC") layer could serve as either the bottom contact of absorber 1, as shown in (c), or the top contact of absorber 2 if polarities are reversed. A p-type semi-TC could also be used in other tandem configurations, such as a window layer in a two-terminal (2T) monolithic tandem; however, in other cases, lateral transport may be less important. (d),(e) Reported demonstrations of p-type TCs in PV devices, in which lateral transport is also less important, are included for reference: (d) a semitransparent bottom electrode or buffer for thin-film solar and (e) hole-transport layers (HTLs) in contact with an n-type TC. (f) A summary of properties that must be attained in each configuration. This figure is intended to represent the key functionalities that p-type TCs could enable and is by no means exhaustive. The layers are simplified for clarity and thicknesses are not to scale.

(3) *First experimental realization*. The material is synthesized for the first time, usually in the form of a bulk single crystal or powders (e.g., using solid-state synthesis or mechanochemical synthesis). From powders or single crystals, it is possible to confirm crystal structure, stoichiometry, air and moisture stability, and preliminary properties, though at this stage optoelectronic properties are not usually assessed. When screening from a database of known materials such as the Inorganic Crystal Structure Database (ICSD), this stage has often already been realized and so occurs before stage 1.

(4) *Thin film synthesis*. The material is synthesized as a phase-pure conformal thin film. There are numerous methods to fabricate thin films, from wet synthesis to chemical or physical vapor deposition, in one or multiple steps. Thin film formation can result in epitaxial (single-crystal), polycrystalline, or amorphous films. The microstructure, thickness, stoichiometry, point or crystallographic defects, and surface effects will strongly influence the thin film properties and functionality. Specific synthesizability challenges and disconnects for p-type TC thin films have been discussed previously by Fioretti and Morales-Masis [38].

(5) *Thin film optimization*. A p-type TC film is optimized, with high transparency and conductivity (the first reported film in stage 4 is usually not indicative of how much performance can be tuned). Such optimization can occur through doping, alloying, or optimizing process conditions such as annealing, among other methods. Throughout this paper, "high" transparency refers to $\alpha > 10^4$ cm^{-1} and "high" conductivity refers to $\sigma > 10$ S cm^{-1}, though what is considered sufficiently "high" depends on the application. We note that this stage is often skipped for novel p-type TCs.

(6) *Junction demonstration*. A p-type TC is demonstrated to form a junction with another material, either deposited directly on an active substrate or

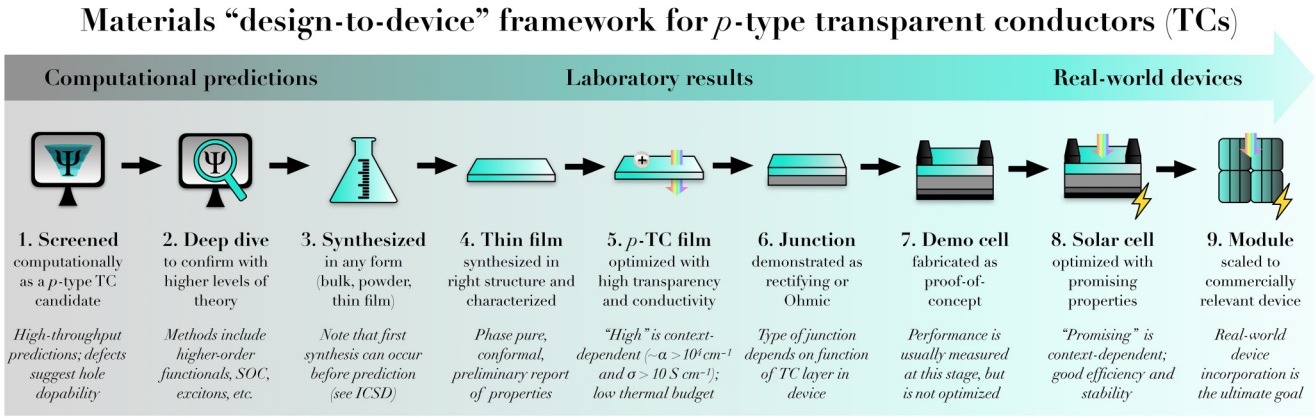

FIG. 3. Our proposed framework of the materials "design-to-device" progression for p-type transparent conductors (TCs), representing stages of technological innovation from computational prediction (far left) to a scalable device (far right). In Fig. 1, we highlight computational methods within the first two stages of this process, while in Fig. 2, we outline various device designs in stages 7–9.

on top of a device stack. The key challenges at this stage are chemical and thermal compatibility (e.g., to avoid chemical intermixing at interfaces or material degradation) and electronic alignment (e.g., valence band energies aligned), as well as good physical adhesion, without degrading the junction partner material.

(7) *Solar cell demonstration*. The p-type TC film is incorporated into a full solar cell device stack with demonstrated performance. Often, this first device has low efficiency and poor device characteristics. p-type TCs can be deposited directly on a substrate or on top of the device stack (depending on the device polarity). The substrate or device stack will define the limitations for the p-type TC film deposition, such as the thermal budget. This in turn will influence (or limit) the final properties of the p-type TC film.

(8) *Solar cell optimization*. The solar cell is optimized around the p-type TC layer, with reasonable PV performance values such as the open-circuit voltage, fill factor, and efficiency. At this stage, in addition to retaining good thin film properties and optimizing the TC, the interfaces play a key role in device performance. One way in which this disconnect can be alleviated is by including interface simulations once the device stack is known (e.g., as done for organic and halide perovskite solar cells) [39].

(9) *Scaling from device to module level*. Scaling up laboratory-scale devices (solar cells) into commercially relevant devices (solar modules) requires different fabrication techniques for TCs and can change properties and requirements. As reported in the well-known PV-efficiency charts compiled by the National Renewable Energy Laboratory (NREL) [40,41], solar cell properties often cannot be reproduced on the module scale, due to various disconnects such as conformality and processing constraints. At this stage, supply chain, cost, and sustainability factors also must all be considered. The ultimate goal of materials discovery is to go from a predicted material to this final stage.

This framework will be used throughout this paper to guide our exploration of disconnects. These steps are inspired by the technology readiness level (TRL) framework, which will also be referred to when appropriate; however, our steps 1–6 expand upon earlier stages of materials design. This framework is designed and adopted specifically to address stages of materials discovery in p-type TCs. We emphasize that discovery does not necessarily follow this linear flow: often, optimization involves iteration between these stages. Historically, most materials have been synthesized first, before computational predictions, and many recent studies return to computational "deep dives" after experimental stages to fill in experimental knowledge gaps or inform decisions. To highlight representative materials discussed throughout this paper, in Fig. 5 we illustrate the stage along the "design-to-device" framework at which research and development is stalled, a graphical highlight of research at this stage and one of the key disconnects describing why progress is stalled.

III. DESIGN-TO-LABORATORY DISCONNECTS

In this section, we outline key disconnects that emerge going from the prediction of a new p-type TC (stage 1) to the realization of optimized properties in an experimental p-type TC thin film (stage 5). Some common disconnects at this stage are summarized in the left-hand side of Fig. 4. We will also discuss strategies to confront these challenges.

We note that "figures of merit" (FoMs) have been used to assess and optimize TCs. However, there have been

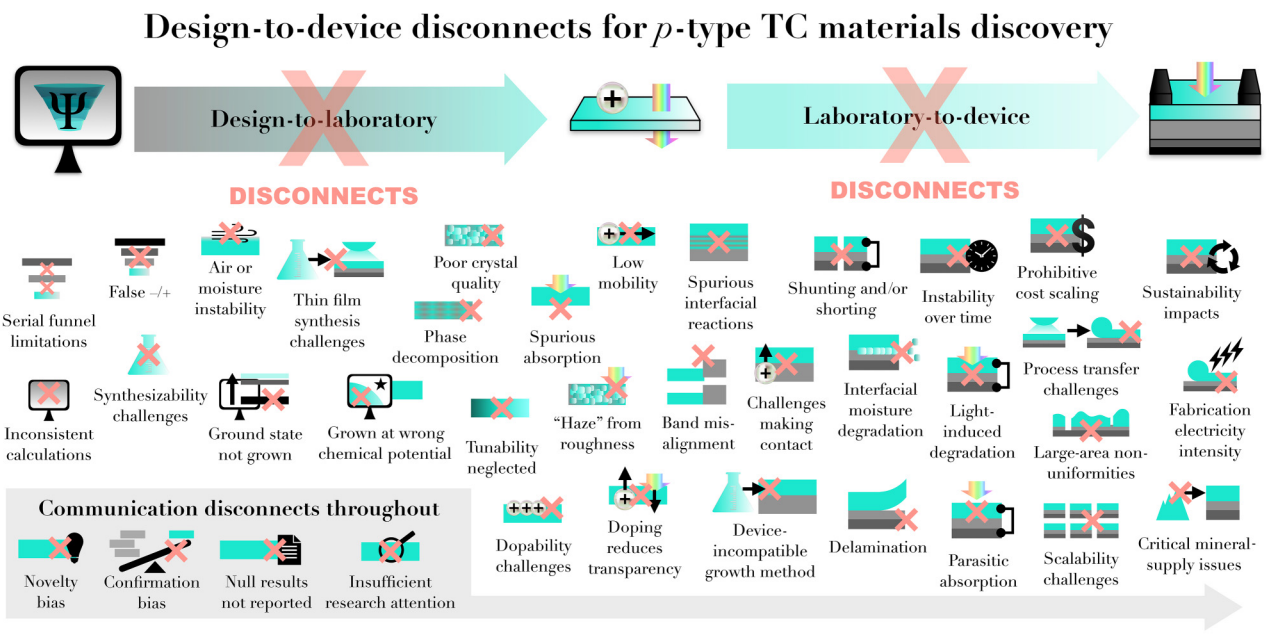

FIG. 4. A schematic summary of the primary disconnects in scaling computationally predicted p-type TCs into solar cell devices.

multiple FoMs proposed ("Fraser and Cook" [42], "Haacke" [43], "Gordon" [44], and "Haacke High Resolution" [45], among others) and there is no consensus in the community as to which is best, in particular for p-type TCs. The selection of an appropriate FoM is highly application dependent and material dependent, with potential for misuse in material selection based on FoMs alone. We caution against using a single generalized application-agnostic FoM, recommending instead to either report optical and electrical measurements separately or define an FoM for a specific application, and therefore we do not report FoMs (see instead reported FoMs from the experimental literature [46–48]).

A. Computational screenings contain limitations and biases

First-principles computations are powerful but have inherent fundamental limits and numerical dangers such as convergence that need to be kept in mind. We will assume in this discussion that computations have been performed by an expert, achieving the necessary numerical convergence for the targeted task. We will also assume that the inherent limits of the approximation used [e.g., semilocal density functional theory (DFT) underestimates the band gap and affects defect computations dramatically] are taken into account in the screening process. Unfortunately, a small fraction of studies in the field do not follow these requirements and we warn the reader to always question whether computational results have been interpreted with caution and the right amount of expertise.

The efficacy of high-throughput computational screenings emerges from the quality of its input data, which usually comes from computational databases or the ICSD. These repositories have grown substantially, encompassing diverse materials and properties. However, extensively studied materials are over-represented in these databases, which can induce a selection bias toward well-studied candidates and can potentially neglect less-studied ones. For example, previous literature suggests non-oxides as promising p-type TCs due to low effective masses and low ionization potentials [11]. However, there are far more oxides than non-oxides in materials databases, so non-oxides are under-sampled in screening studies.

An algorithmic bias can lead to prioritizing properties that are more readily calculated or accessible, potentially overlooking properties that may be more representative of desired performance. In order to reduce the input materials to a manageable subset, the initial steps of computational screenings usually filter with property proxies that are computationally inexpensive ("cheap") to calculate. For example, although both effective mass m^* and scattering time τ contribute to achieving high mobility, given current algorithms m^* ("cheap" proxy) is much easier to calculate than τ ("expensive" proxy). Additionally, hole conductivity depends on doping density, which is also difficult to compute. Therefore, we are biased toward looking for materials with low m^* rather than those with excellent scattering or doping properties and we need to be careful about how close a cheap proxy correlates to an expensive proxy.

Similarly, a knowledge bias occurs when a model or analysis is limited by existing knowledge and fails to

account for emerging or unexplored factors. For example, screening for low effective mass and a wide direct band gap as shown in Fig. 1(a) is appropriate for traditional TCOs that behave as doped semiconductors following a rigid band model (e.g., ZnO and SnO_2). More recently proposed mechanisms such as polaronic TCs [9], intrinsic TCs [49], or TCs containing forbidden transitions [30] are less likely emerge from this approach; however, this can be remedied when new mechanisms are understood and can be incorporated into the screening.

Once screening criteria are chosen, a threshold bias can arise from selecting cutoffs, their tolerances, and criteria priorities, as these thresholds often lack objectivity. For instance, picking a cutoff for "low" hole effective mass (m_h^*) is typically arbitrary; opting for only the lowest m_h^* could exclude highly transparent materials and the m_h^* needed to achieve a certain high mobility depends on material physics. Additionally, there is a lack of threshold standardization regarding how defect calculations are performed and interpreted. While serial screening is common, Pareto analysis or multiobjective optimization can counter threshold bias and improve outcomes [50]. However, one key challenge is to select appropriate weighting parameters formally and quantitatively. Such optimizations become application dependent and are rarely done for p-type TCs.

Lastly, biases can occur when reporting computational results. Novelty biases can lead to publishing and highlighting new and exciting findings, while negative or non-novel outcomes are not usually reported. Screening studies tend to report "new" p-type TC predictions rather than reporting whether past predictions have been corroborated. However, especially given challenges to synthesizing predictions in the laboratory (see the next sections), it would be extremely useful for experimental researchers to know whether a result has been computationally reproduced by multiple groups and different methods. One approach could be to establish an open computational database specifically for p-type TCs to enable comparison of calculation parameters and results; such an effort would require dedicated funding and staff for development and maintenance.

Together, these biases can lead to false negatives and false positives emerging from screenings. Input sets and screening criteria need to be judiciously selected and appropriately communicated to avoid misleading predictions. Although false negatives are challenging to address, false positives can be mitigated by performing a computational "deep-dive" (stage 2) before attempting synthesis. As an example from our research, shown in Fig. 5, sputter synthesis was attempted (stage 3) shortly after $ZnZrN_2$ emerged from a p-type TC screening (stage 1), before a thorough computational assessment (stage 2). The target phase could not be synthesized, and by turning back to a "deep dive," it was hypothesized that due to disorder intolerance the selected synthesis method would likely have never yielded this phase [51]. In general, experimentalists using screenings to inform their research should be aware of how such biases propagate and how to carefully scrutinize the extent of computational findings before going to the effort to grow it in the laboratory.

B. Predicting synthesizability and stability can be challenging

1. Bulk crystal synthesis

The next disconnect is that many new p-type TCs have been predicted but not all have been successfully synthesized in the laboratory in the desired crystal structure (stage 3 in Fig. 3). One likely reason for the lack of reported synthesis is that many have not been attempted yet, or if attempted have not been published possibly due to negative results (so-called "dark reactions" [52]). Computational databases tend to report whether a given material has been synthesized previously (pointing to the ICSD) and bulk or powder synthesis is most common. One approach to avoid assessing synthesizability is to simply restrict input data sets to just these known experimental materials. However, some exciting new predictions of p-type TCs do not yet have any reports of synthesis, e.g., $CsMCh_2$ (Ch = S, Se, Te) [18] and double perovskites such as $Cs_4M^{2+}B_2^{3+}X_{12}^{VII}$ [53], so for these materials synthesizability should be judiciously assessed. We will start by discussing challenges that have arisen with growing hypothetical crystals that have not yet been synthesized in any form.

Accurate assessment of whether a hypothetical material is actually synthesizable and stable is not trivial. The first disconnect arises from the crude assumption that the descriptor E_{hull} is a good proxy for synthesizability. Namely, it is generally assumed that materials with formation enthalpies at or near the ground-state energy predicted by DFT at 0 K ($E_{hull} \simeq 0$ eV/atom) are the most likely to be experimentally realized, while materials with $E_{hull} \gg 0$ eV/atom are less likely to be synthesized [54–56]. E_{hull} itself is impacted by errors in DFT and correction schemes and does not include entropic effects. Various low-cost approaches to estimate vibrational and configurational entropy have emerged [57,58], which can be incorporated into future screenings. Additionally, assessing dynamic stability is essential [59] and synthesis is driven by kinetics as well as thermodynamics. Despite many recent first-principles and machine learning (ML) efforts to address kinetics via synthesis pathways [60–65], such as solid-state reaction networks [66,67], a deeper understanding and predictability is still needed. Increasing efforts in automating solid-state synthesis may help address this challenge, through solution-based approaches such as robotic arms to handle chemical synthesis as well as various high-throughput vacuum-based approaches [61, 68,69]. To our knowledge, autonomous laboratories have

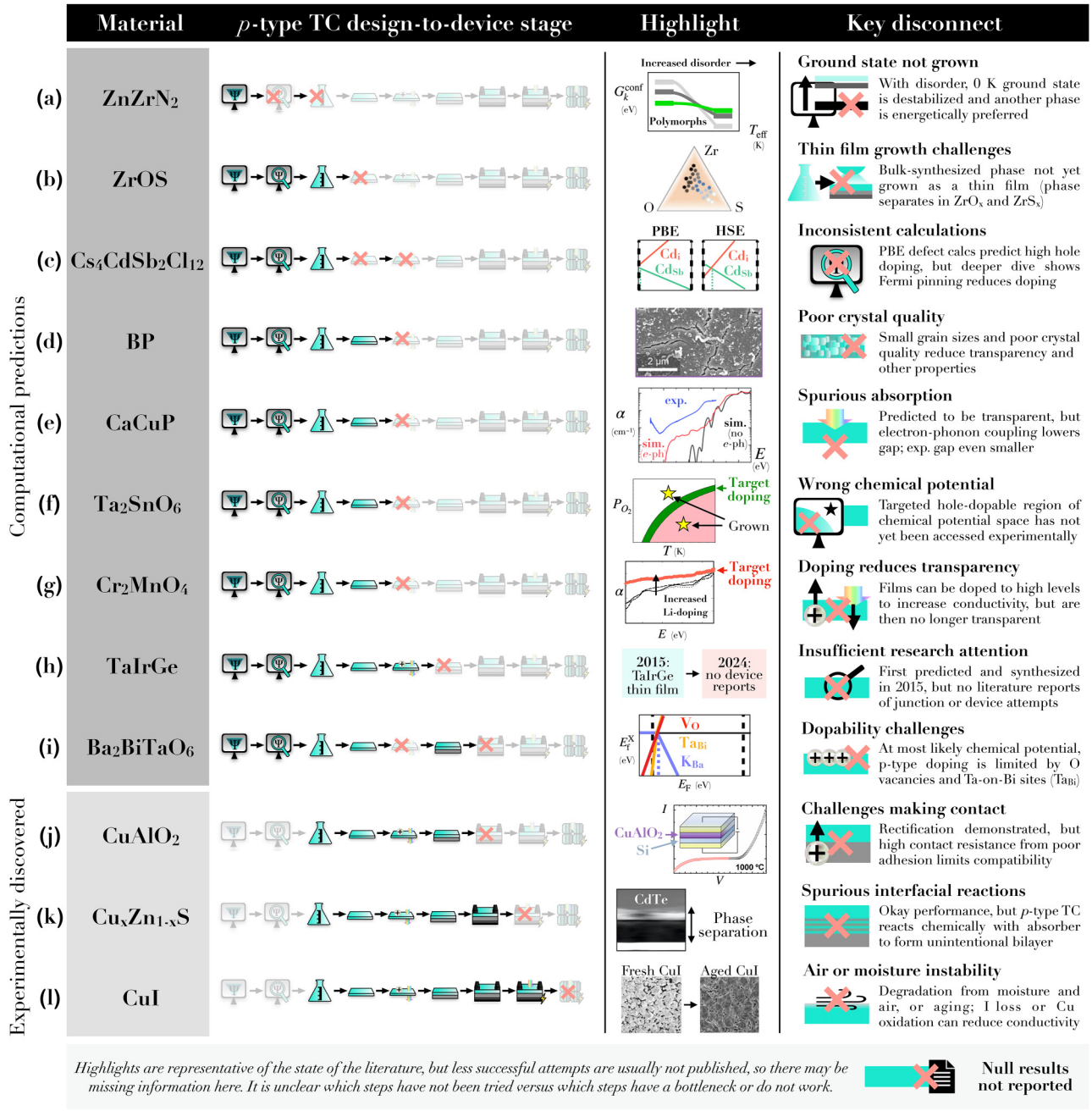

FIG. 5. Examples of proposed and realized p-type TC candidates across the stages of their development process (as outlined in Fig. 3). Materials (a)–(i) have been predicted computationally, while materials (j)–(l) were discovered first by synthesis and are included here as references. The materials are included as follows, with the "highlight" column containing key results adapted from figures from the literature: (a) $ZnZrN_2$ (Woods-Robinson *et al.* [51]), (b) ZrOS (adapted with permission of Monica Morales Masis, from Fioretti and Morales Masis [38], copyright 2020, SPIE), (c) $Cs_4CdSb_2Cl_{12}$ (Hu *et al.* [114]), (d) BP (Crovetto *et al.* [28]), (e) CaCuP (Willis *et al.* [80]), (f) Ta_2SnO_6 (adapted with permission from Barone *et al.* [29] copyright 2022, American Chemical Society), (g) Cr_2MnO_4 (Nagaraja *et al.* [115]), (h) TaIrGe, (i) Ba_2BiTaO_6 (adapted with permission of Geoffroy Hautier, from Dahliah *et al.* [116], copyright 2020, Royal Society of Chemistry), (j) $CuAlO_2$ (Ling, *et al.* [117]), (k) $Cu_xZn_{1-x}S$ (Woods-Robinson, *et al.* [118]), and (l) CuI (Raj, *et al.* [119]). The permissions have been conveyed through the Copyright Clearance Center, Inc., and all other figures have been adapted from a license with reuse permissions. Details of the highlighted figures and the corresponding data tables are included in the Supplemental Material [34].

not yet been tailored toward p-type material discovery but could be a promising research direction, especially for exploring processing conditions to promote phase stability and optimizing dopants and off-stoichiometries.

Specific synthesizability challenges can arise due to the complexity of compounds selected as p-type TC candidates [70]. Many predicted TCs are multinary materials, since multiple elements provide an increased search space and tunability [71]. For instance, $CuAlO_2$ (often considered the first p-type TC) can be considered a ternary extension to p-type Cu_2O in which introducing Al increases the band gap [72] and, similarly, Ba_2BiTaO_6 a quaternary extension of p-type $BaBiO_3$ in which Ta increases the gap. Furthermore, binary TCs can be extended into multinary solid solutions to enhance performance, such as recent S incorporation into CuI [47,48,73]. However, adding more elements can induce challenges in synthesizability, including increased likelihood to phase segregate, as well as complex disorder and defect configurations [56,70]. For example, one challenge that has stalled progress in thin film synthesis of predicted p-type TC ZrOS [10] has been phase separation into defective binary phases ZrO_x and ZrS_x, as it is challenging to introduce S into ZrO_x (see Fig. 5) [38]. Another well-known example of such challenges can be observed in quaternary and quinternary kesterite PV absorbers, which tend to easily phase separate [74].

Even if reported as "synthesized" in the ICSD, many compounds are not stable in air or moisture. For example, $K_2Sn_2O_3$ was predicted as a p-type TC by Hautier *et al.* [10] but rapidly degrades in air. Air instability does not completely rule out a candidate but using such materials in a device and even measuring them introduces serious challenges. For example, SnO and AgI are unstable in air but have still been explored for device applications. CuI can also present stability challenges when exposed to air and moisture, presenting variations in conductivity due to iodine loss or Cu oxidation. However, this depends strongly on the fabrication method and solar cell process used [75–77]. Non-oxides in particular tend to be less stable in air and moisture; some are protected by a passivation layer, while others can fully decompose or oxidize. One simple thermodynamic check for moisture instability is the descriptor "energy above the Pourbaix hull" (E_{pbx}), based on Pourbaix diagrams [78]. Another recent method uses a "greedy algorithm" to assign heats of oxidation to screen for in-oxygen environmental stability and heuristically determine whether a material may self-passivate [79]. However, to our knowledge there is no extensive benchmarking to show that these metrics are predictive of experimental instabilities. In our experience, especially with non-oxide TCs, p-type TC candidates predicted stable by E_{hull} and even E_{pbx} have still degraded in air. Air instability may be a key reason why progress in non-oxide p-type TCs has been limited.

2. Thin film synthesis

Specifically for TCs, another set of disconnects arises going from bulk synthesis to thin film synthesis (stages 3 and 4). Computational predictions are generally derived from bulk periodic calculations at thermodynamic equilibrium, whereas in practical applications p-type TC materials are thin films, contain multiple types of defects, and are usually synthesized using nonequilibrium growth techniques. Sometimes these assumptions hold and, e.g., a predicted structure can be grown as a thin film with properties corresponding to predictions, as demonstrated by various success stories such as Ba_2BiTaO_6 and CaCuP [15,80]. However, this is not always the case; the effects of surface energies, surface termination, strain, and texturing in thin films can influence which phase is stabilized at a given condition and can yield a range of properties far beyond the single observable value predicted for the bulk structure. Additionally, amorphous thin films are difficult to simulate, though many high-performing n-type TCs are amorphous [55].

Similarly, different thin film synthesis methods can result in an extensive span of structural properties that can deviate from predicted bulk properties. However, there is not yet a framework such that an ideal synthesis route and tool can be selected from first principles alone. The synthesis pathway prediction algorithms mentioned previously are a step in this direction, but these assume thermodynamic equilibrium and are method agnostic (many polycrystalline thin film synthesis methods are nonequilibrium). From the experimental side, the synthesizability challenge is to grow thin films that can tolerate defects in microstructure, surface effects, grain boundaries, strain, dislocations, etc., while retaining properties simulated from single-crystalline materials (see Sec. III C) [12]. In sputtering, a technique commonly used for exploratory synthesis as well as for commercial TCOs, in some cases the "effective temperature" at the surface of a growing film has been shown to be more predictive of synthesizability and structural properties, rather than the chamber temperature [51]. One disconnect here is simply that in stages 3 and 4, not all synthesis pathways have been sampled. Confirmation biases can arise if researchers try one approach, encounter difficulties, and then decide to abandon the material altogether without exploring alternative approaches to access a different region of configuration space.

C. Origin of the mismatches between theoretical and experimental optoelectronic properties

If a predicted p-type TC can be successfully synthesized as a thin film (stage 4), the next challenge (stage 5) is to experimentally achieve predicted properties of interest such as high optical transparency and high hole mobility and concentration. Yet in some cases of predicted p-type

TCs grown in the laboratory, at least one of these properties falls short of the computationally predicted ideal. There may be three reasons for these disconnects: (1) limitations of high-throughput descriptors in accurately estimating the optoelectronic properties, (2) differences in material properties between an ideal bulk crystalline material (the object of computational modeling) and a practically realizable thin-film material, and (3) extrinsic experimental issues negatively influencing the predicted properties of a thin-film material.

1. Accuracy of high-throughput optoelectronic properties

First-principles calculations are useful to approximate experimental properties but they also come with caveats. In general, more "expensive" calculations improve accuracy but there are still limits and trade-offs. Rather than review computational methods to screen for *p*-type TCs, which has been done in depth elsewhere [2,12,13,81], here we will highlight a few key limitations to computing transparency, mobility, and dopability in bulk crystalline materials. We note, however, that the most efficient high-throughput approaches are built using a tiered screening approach, where cheap methods are used first to select materials (taking into account their lower accuracy) and more accurate and expensive methods are used for the final candidates before moving up to experimental verification (see Fig. 1).

A wide band gap is a central property of a TC. While "traditional" semilocal DFT is known to significantly underestimate band gaps (sometimes by 1–2 eV) [82], many more accurate methods with different levels of costs are available nowadays, such as *GW* or hybrid functionals [9]. Some of these methods have already been used in a high-throughput fashion and ML is speeding up the assessment of high-accuracy band gaps with minimal computational cost [36,83–85]. Beyond the accuracy of the method, one needs to keep in mind that optical gaps are not electronic gaps. A better estimate of the optical gap can be obtained using relatively cheap independent particle approximation (IPA) computations on top of DFT or hybrids. These computations will take into account the transition dipole moment for optical absorption (i.e., the oscillator strength) with possible forbidden or weak transitions. Some important TCs such as In_2O_3 rely on forbidden transitions for their high transparency [86]. Recent high-throughput work including in the TC field has started including these optical absorption computations and *p*-type TCs with forbidden transitions have recently been proposed [30]. We note that more expensive approaches beyond IPA such as time-dependent DFT (TD-DFT) or Bethe-Salpeter equations (BSE) can be used to provide more accurate optical absorption but, in general, TCs with a band-like conduction mechanism have effective masses and band gaps that lead to small excitonic effects (exciton binding energies of around the tens of millielectronvolts) [87].

To model transport, effective masses (m^*) that can be obtained from DFT or higher-order theories are most commonly used as a proxy for carrier mobility. While effective masses vary between semilocal DFT and more accurate methods, the difference is usually small enough for semilocal approaches to suffice, especially when using m^* for screening and as a proxy for mobility. While m^* is a simple concept for conventional single-parabolic band materials, real materials can be anisotropic and have complex band structures with several competing bands [9]. Discrepancies between computed values of m^* for the same material in the literature often come from different crystallographic directions or bands. When used as a proxy for mobility, it is important to consider all the possible bands involved in transport and average them out. Otherwise, picking the highest-curvature band tends to underestimate the effective mass. In the past five years, the full computation of mobility has made enormous progress. Codes such as PERTURBO [88], EPW [89], and ABINIT [90] have well-documented and tested open-source codes that fully compute phonon-limited mobility. These comprehensive approaches have been even scaled up and can be used to compute hundreds of materials automatically [91]. They remain expensive, however, and simpler approaches assuming simplified scattering processes have emerged, such as AMSET, which also provides a high-quality open-source code [92]. Errors of around 20% compared to experimental mobilities have been reported for these approaches based on electron-phonon and Boltzmann transport theory [92]. The field of TC design has already started to use these methods in recent studies [23,30,32,80,93].

Finally, defects are essential to understand and predict *p*-type TCs. Point defects control doping and intrinsic defects can prevent *p*-type doping. Certain defects (e.g., oxygen vacancies) can act as "hole-killers" and prevent *p*-type doping. Due to the lack of automation and high computational cost, early high-throughput studies only computed defects as a "deep-dive" step after low-m_h^* and wide-band-gap materials had been identified [10]. However, since then, automation has made huge progress and software packages such as PYCDT and PYLADA have emerged that facilitate the generation and processing of input and output files (including charge corrections) [94,95].

Nowadays, key challenges stem not from automation but, rather, from the compromise between expensive large supercell computations with hybrid functionals (which is the gold standard for defect computations) and the cheaper semilocal DFT-based approaches. While semilocal DFT can provide important information and has helped in first-stage screenings [37], it remains essential to always verify these crude methods with a hybrid functional, at

the very least for the most promising materials. Indeed, similar to how semilocal DFT underestimates band gap, it tends to overpredict dopability and its use without safeguards has led to false predictions of p-type doping. One pertinent example from the literature is the case of $Cs_4CdSb_2Cl_{12}$, one of a new class of quadruple perovskites initially predicted in 2018 as p-type TCs using DFT defect calculations without hybrid confirmation [53]. However, when $Cs_4CdSb_2Cl_{12}$ was synthesized the following year, p-type doping was not achieved; these authors fact-checked theoretical dopability using a hybrid HSE functional and the results suggested that these materials were not actually highly p type, with doping limited by Cd interstitials (see the schematic defect formation-energy diagrams in Fig. 5) [96]. In response, the authors of the original study then performed follow-up hybrid calculations and revisited their original claim: $Cs_4CdSb_2Cl_{12}$ could indeed be highly p type but only within a specific region of chemical potential space (Cl-rich and Cd-poor, with fast quenching during growth) [97]. To our knowledge, doping within this region still awaits experimental confirmation.

The field of high-throughput defects is moving fast, with interesting developments in the use of methods compromising between DFT and full hybrid, such as single-shot hybrid, as well as work on the more exhaustive search of the defect energy landscape [98–100]. In all cases, defect computations remain expensive and proxies have been highly sought out. Some recent studies have applied practical single-defect-based descriptors early in the screening, such as the hydrogen interstitial defect descriptor ("FEH") [21] or the oxygen vacancy formation energy descriptor [101]. Other studies have used branch point energy (BPE, or E_{BP}) as a descriptor [16,18] but we caution against using BPE as its predicting power is questionable [12].

2. Thin film properties can diverge from bulk properties

Practical TCs are normally required in the form of thin films with thicknesses on the order of a few hundred nanometers. Even if bulk properties are appropriately modeled and if thin films can be grown, this requirement generates another possible source of disconnects between calculated and experimental properties (stages 4 and 5 in Fig. 3). Most first-principles materials modeling methods assume a perfectly crystalline and infinitely periodic material. However, both assumptions often break down in thin film TCs, where nonequilibrium effects (e.g., nonequilibrium defects and solubility, strain and surface tension, substrate effects, influence from plasma, etc.) and nanoscale effects (e.g., grain-boundary scattering, amorphous effects, and quantum confinement) can dominate [102].

Depending on the substrate and on the growth process, thin films can be epitaxial single-crystalline, epitaxial polycrystalline, nonepitaxial polycrystalline, and amorphous. Moving down this list, an increasing deviation from the properties of bulk single crystals is typically observed. The current generation of n-type TCs is either nonepitaxial polycrystalline [ITO, Al-doped ZnO (AZO), F-doped SnO (FTO)] or amorphous [Indium gallium zinc oxide (IGZO), zinc-tin oxide (ZTO), indium-zinc oxide (IZO)] [103]. Therefore, it is unlikely that epitaxial single-crystalline films can practically be used as p-type TCs, both because of the much higher cost and the requirement of a suitable substrate, which is usually dictated by the application (see Sec. IV C).

The TC-relevant property that is most often affected by imperfect crystallinity is carrier mobility. At a hole concentration of 10^{18} cm^{-3}, single-crystalline silicon has a hole mobility of about 200 $cm^2\ V^{-1}\ s^{-1}$, whereas the mobilities in polycrystalline Si with 120-nm and 23-nm grains are about 10 $cm^2\ V^{-1}\ s^{-1}$ and 1 $cm^2\ V^{-1}\ s^{-1}$, respectively [104]. At an electron concentration of 10^{19} cm^{-3}, typical electron mobilities of ZnO are 70 $cm^2\ V^{-1}\ s^{-1}$ for single crystals, 40 $cm^2\ V^{-1}\ s^{-1}$ for epitaxial films, and below 1 $cm^2\ V^{-1}\ s^{-1}$ for nonepitaxial polycrystalline films [105]. While the relative importance of grain-boundary scattering decreases with increasing carrier concentration, grain-boundary scattering can still remain a mobility-limiting mechanism even in the 10^{21} cm^{-3} carrier concentration range [105], so it is relevant for TCs. The lower mobility of nonepitaxial polycrystalline films with respect to their epitaxial counterparts can also be due to a higher density of both point defects and extended defects. These considerations do not invalidate the screening approach, with the understanding that the computationally determined mobilities are generally upper bounds for the mobilities achievable by polycrystalline thin films. Large crystalline bulk mobility is a necessary but not sufficient requirement, as grain-boundary scattering could be an issue [106,107]. Although grain-boundary scattering is difficult to model from first principles, various simplified high-throughput approaches have been proposed and applied [92,108,109], and including it in screenings could be an interesting future avenue of research.

Another property that can be affected by imperfect crystallinity is optical transparency, especially when the fundamental band gap of the material is indirect and located at visible (rather than UV) wavelengths. In these cases, the applicability of the material as a TC relies on the weakness of indirect optical transitions, resulting in negligible absorption in a thin-film sample because transitions involve both a photon and a phonon. Deviations from perfect crystallinity due to, e.g., closely spaced grain boundaries, extended defects, and inhomogeneity, are expected to relax the requirement for phonon participation in these transitions and, hence, increase the absorption coefficient of the material. The increase in the absorption coefficient of silicon between its indirect and direct band

gap with decreasing crystalline quality is a well-known example [110]. A similar effect has recently been observed in polycrystalline BP and CaCuP films, predicted p-type TCs with direct gaps much larger than indirect gaps (see the absorption spectra of CaCuP in Fig. 5) [28,80]. In both cases, the experimentally reported absorption coefficient in nanocrystalline films is much higher than the calculated absorption coefficient using hybrid functionals and electron-phonon coupling, rendering them nontransparent, and an example of poor crystal quality in BP is depicted in Fig. 5.

Due to the requirement of inexpensive large-area thin-film samples for TC in PV applications, such nonidealities might be unavoidable in practice. One may argue that some detrimental effects of polycrystallinity may vanish for large crystal grain sizes in the micrometer range, which can often be achieved in thin film samples, including In-based TCOs [107]. For some TCs, such as ZnO, FTO, and large-grained CuI, optical scattering effects typically become more prominent with increasing grain size due to an increase in surface roughness. This is visually manifested as a "haze" effect, which can be beneficial in thin-film PV devices for light management but could also result in low transmittance [111]. For reference, the grain size of commercial ITO films (n-type TCs) is often below 30 nm [112,113].

One overarching disconnect between bulk and thin film materials follows from the fact that many thin film growth techniques operate under strongly nonequilibrium conditions, where thermodynamics-based modeling methods may not be appropriate. Some examples are plasma-based techniques such as sputter deposition, pulsed laser deposition, and plasma-assisted chemical vapor deposition. Interestingly, these are some of the most commonly used deposition techniques for TCs, partially because the presence of energetic species in the plasma can promote higher dopant solubility at low temperatures. In these types of processes, where both ions and neutral species are present with a range of energies, the atomic chemical potentials used in the calculations of defect formation energies are not easily translated to experimental process conditions. Thus, the dopability of a TC may be significantly different than expected. The mobility may also be affected, since it is often limited by defect scattering in highly doped materials.

3. Challenges optimizing thin film growth and defects

Early synthesis attempts usually result in low-quality properties, which can be optimized and tuned with increased research efforts. For example, in the first reports of thin film n-type ITO in the 1970s, the conductivity was approximately 300 S cm^{-1} [120], but after two decades of intensive research, the conductivity was optimized to nearly 2 orders of magnitude higher (with a record of approximately 22 000 S cm^{-1} [121]). Since most of the predictions of p-type TCs have been within the past decade and a given prediction has received far less attention than ITO, it is reasonable that the development of predicted TCs that have been grown as thin films is stalled between stages 4 and 5 in Fig. 3.

Growing a high-performance p-type TC requires optimal control of growth conditions and thus chemical potentials. Many of the computationally identified candidates offer p-type doping only within a specific window of chemical potential. For instance, a well-adjusted oxygen chemical potential can be essential during growth, since highly reducing conditions can create oxygen vacancies that compensate any holes. We note that this problem can be present even if an shallow acceptor is incorporated in the film. Ba_2BiTaO_6, for instance, shows limited p-type doping because of the presence of oxygen vacancies (V_O) and Ta-on-Bi antisites (Ta_{Bi}), as shown in the defect formation energy diagram of Ba_2BiTaO_6 in Fig. 5 (adapted from Dahliah *et al.*) [116].

While computational screening uses some level of dopability, screening leads us to focus only on materials that could potentially be p-type doped (i.e., that could exist in chemical potentials that are favorable for hole doping). There is not an easy relation between chemical potential and experimental growth conditions. While qualitative statements can be made—i.e., a lower oxygen chemical potential will be obtained by working in a reducing atmosphere—computations cannot tell what exact conditions (gas flow, temperature, etc.) to use experimentally. The computed chemical potential can be influenced by effects not taken into account (alloying and unknown phases or temperature effects). Similarly, source-material impurities should be carefully checked; e.g., C and Si are dominant impurities in boron sputter targets but are some of the most effective dopants in BP (Si impurities alone can lead to carrier concentrations 10^{19} cm^{-3} [28].)

Any single growth technique will have limits in terms of attainable chemical potentials. A recent case in point is the growth of Ta_2SnO_6 [29], which has been computationally identified and reported as a potential p-type TCO (albeit with a small gap of 2.4 eV) and is highlighted in Fig. 5 [114,122]. High-quality single crystals grown by molecular-beam epitaxy (MBE) did not yield any measurable conductivity, even after extrinsic doping attempts using K and Ti. The most likely reason for these failed doping attempts lies in the limits of the oxygen chemical potential achievable in MBE. Oxygen vacancies act as hole-killers and need to be avoided under oxidizing conditions. However, the most oxidizing conditions available with this MBE process are still not oxidizing enough to enable p-type doping. It remains to be seen if other growth techniques will lead to p-type doping in Ta_2SnO_6 and similar effects likely occur in other p-type TC candidates.

For potential TCs belonging to non-oxide families, a common experimental challenge (besides air stability,

discussed earlier) is to ensure low levels of oxygen contamination in the films. This issue is particularly difficult to address when the target TC material contains highly oxophilic metals, such as the ones from groups I, II, III, and IV, and Al. To address this problem, we recommend including "oxygen-tolerance" calculations of promising TC materials, i.e., the calculated formation energy of oxygen substitutional and interstitial defects as a function of the Fermi level. If any of these defects is found to be a donor with low formation energy, oxygen contamination is likely to limit the p-type dopability of the material. The development of more general oxygen-tolerance principles would also be welcome. For example, one may expect that oxygen substitution on the anion site is a donor defect in pnictides (one more valence electron) and an acceptor in halides (one less valence electron). If this is correct, oxygen incorporation would be detrimental for p-type conductivity in pnictides but it might be benign or even beneficial in halides. Beneficial effects of oxygen incorporation have been shown for CuI [77,123]. Furthermore, the formation energy of these substitutional defects might generally be lower in materials containing an anion with a similar ionic radius to O^{2-}. Thus, one may intuitively expect nitride p-type TCs to be most negatively affected by oxygen contamination [124].

As alluded to with these examples, optimization of TCs often involves introducing defects, disorder, and off-stoichiometry in a tunable manner. Sometimes intrinsic doping is possible but usually extrinsic dopants are needed to increase dopability. While most screenings include some consideration of dopability, often only intrinsic defects are considered and detection of problematic hole-killers is targeted without providing the exact shallow dopant to use. However, in some cases dopants have been proposed, e.g., for La_2SeO_2 (Na) [16], BP (Mg, Si, Be, and C) [11], Ba_2BiTaO_6 (K) [116], and CsCuO (Na, K, and Rb) [101]. Our experience is that defect compensation is often more limiting than the discovery of a shallow acceptor. There are a few rare cases in which, even if a material does not have strong compensation, issues still arise in discovering the ideal dopant (e.g., n-type $La_2Sn_2O_7$ [125]).

Moreover, defects and other impurities can influence absorption. Doping to degenerate levels can induce free-carrier absorption in TCs, reducing transparency of materials to long-wavelength photons. Often, computational predictions target perfect stoichiometric materials but promising undoped p-type TC candidates may result in trade-offs in properties upon doping, resulting in false positives. For example, an early screening study predicted Cr_2MnO_4 as a promising candidate and selected Li as a p-type dopant [14]. Synthesis of Li-doped Cr_2MnO_4 thin films indeed yielded p-type conductivities (though only up to 0.035 S cm^{-1}) but at high doping transparency is significantly reduced due to absorption of photons with energies below the band gap, as shown in Fig. 5 [115]. Recent computational studies have proposed computational methods to estimate plasma energy as a function of hole concentration [126]; however, methods to assess the impact of doping on transparency have yet to be implemented in high-throughput screenings.

Likewise, although screenings usually identify ordered compounds, the best known experimental TCs are off-stoichiometric solid solutions rather than dilutely doped compounds. For example, ITO is approximately 5–10 at.% tin, exceeding the dilute limit [127], and the Al content in AZO is approximately 2% [128]. One workaround is to screen for cases in which a solid solution of the two compounds is amenable to high transparency. We have proposed this framework previously and incorporated an "alloys database" tool to do so in the Materials Project [129]. Additionally, in some cases, TC properties could emerge nonlinearly from tunability. For example, in p-type $NiCo_2O_4$ spinels [130], disorder has been shown to reduce the hopping barrier and actually lead to increased conductivity compared to that of the ordered structure [131]. Finding methods to appropriately model and screen for dopants and tunability early on (stages 1 and 2) rather than during experimental optimization (stage 5) could lead to p-type TC breakthroughs, but this has not yet been done in practice.

D. Novelty bias and confirmation bias

Conventional n-type TCs such as ZnO, ITO, etc., have had their growth techniques and properties fine tuned over decades by international research teams and industries for numerous applications. Thus, it is unsurprising that the first results of a new predicted material may not have properties comparable to predictions. But although it is unfair to compare a preliminary result with a highly optimized result of n-type counterparts, this is still often done and may lead to discarding a promising material that just requires optimization to show its real potential. Even if the target material is not synthesized in a particular study, this does not preclude the possibility of synthesizing these compounds using other techniques. Yet null results are usually not reported. This limits the ability for follow-up research to learn lessons from less successful results and for results to be reproduced to increase statistical significance, while increasing the chance of repeating mistakes and wasting resources. We have highlighted a few key exceptions; e.g., Barone *et al.* reported being unable to synthesize conducting phases of Ta_2SnO_6 [29] but this report inspired follow-up calculations to suggest their MBE growth did not sample optimal chemical potentials [132]. To remedy this, amorphous Ta_2SnO_6 has been proposed [132] and these studies inspire future work to explore different regions of phase space.

The initial synthesis of novel computationally identified thin-film materials often entails suboptimal growth

conditions, such as chemical potential. This is particularly true for so-called "high-risk" novel materials, in which customized tools likely do not yet exist, necessitating makeshift adaptations of existing experimental tools. Often, growth chambers designed and previously (or concurrently) used for conventional materials such as oxides are repurposed for the synthesis of multiple new materials. Such adaptations raise concerns about contamination, especially by volatile species such as alkali metals, zinc, sulfur, or halogens, which can compromise the synthesizability of the material, its quality, and its defect sensitivity. For example, growing p-type phosphide TCs in chambers also used for sulfides may adversely affect hole concentration. "Exploratory" tools such as combinatorial sputter chambers can offer a wide range of elements and tunability [133–137], so they are particularly advantageous at stage 4 in Fig. 3. However, exploratory thin film growth chambers accommodating volatile species are not particularly widespread, which is a barrier to enabling synthesis of new predicted p-type TCs. Often when predictions are made, one of the limiting factors is the ability to find a synthesis team willing to risk attempting a novel compound with possibly exotic elements. In spite of these challenges, new high-throughput synthesis methods are on the rise and could enable faster progression from a predicted TC (stage 1) to an optimized thin film (stage 5) [64,138,139].

IV. LABORATORY-TO-DEVICE DISCONNECTS

If a predicted p-type TC can be optimized to high performance in the laboratory, incorporating this material into an actual device will bring a set of new disconnects, some of which are summarized and schematically depicted on the right of Fig. 4. Due to intrinsic disconnects from stages 1–5 and new interface challenges, so far very few predicted p-type TCs have been successfully reported as junctions and in solar cells (stages 6–9 in Fig. 3). For example, although TaIrGe was predicted and synthesized in 2015 as a thin film with high transparency and hole conductivity [26], nearly a decade later, we are unable to find any reports of TaIrGe-based junctions or PV devices, suggesting either insufficient research attention or device attempts that have not been published (see Fig. 5).

Not only are device reports of predicted TCs rare but we were unable to find reports of *any* p-type TC included as a layer for lateral hole transport, i.e., "electrode" in Figs. 2(a)–2(c), even as a small-scale proof-of-concept cell (stage 7). Although p-type Ba_2BiTaO_6 has been demonstrated as a p-n junction diode with n-type $SrTiO_3$ (see Fig. 5) [25], demonstrating carrier transport and device potential, to our knowledge it has not been grown in a PV device. The only exceptions are NiO_x, which is not technically a p-type TC due to low hole conductivity (although a recent report has suggested that external dopants could increase hole transport [140]), and Cu_xS, which is not very transparent, and in both cases devices have very low efficiencies [141]. From our understanding, p-type TCs have only been reported in solar cells as out-of-plane transport layers stacked next to n-type TC electrode or as continuous metal layers, as in the HTL of Fig. 2(d), or as a semitransparent bottom contact, as in Fig. 2(e).

With these limitations in mind, in this section we reflect on some lessons learned from reported attempts to incorporate p-type TCs into PV-relevant devices as HTLs, generally following the device configuration shown in Fig. 2(e). We use insights from several p-type TCs which were first discovered experimentally, such as $Cu_xZn_{1-x}S$, CuI, and delafossites $CuMO_2$, as well as common non-TC hole-transport materials (HTMs) such as NiO_x and common n-type TCs (see Fig. 5). Our expectation is that insights will be transferable to computationally predicted TCs once they can be optimized and that when advances in material properties are achieved (stages 1–5), understanding these insights will enable more rapid scale-up into PV devices (stages 6–9).

To illustrate the variety of p-type TC contact materials that have been recently incorporated into PV devices, and the magnitude of research efforts as well as what is currently lacking, in Fig. 6(a) we depict a set of inorganic p-type TCs from the experimental literature that have been implemented as electrodes or HTLs in perovskite solar cell devices (NiO_x is included as a benchmark). The data sets used to configure this plot have been processed from the open-access Perovskite Database [141]. For each reported cell, the shading indicates whether it is are part of a double-layer top-contact HTL stack, a double-layer back-contact HTL stack, or a single-layer top electrode; notably, only two binary materials have been reported as a top electrode and therefore this is an area for future research. Perovskite cells have been selected here as representative since the search for HTLs is an active area of research and therefore many p-type TCs have recently been attempted; we acknowledge that the high hole mobility requirement of p-type TCs is not usually needed for HTLs (and some do not need very high transparency), so this test case represents a specific subset of TC design criteria.

In Fig. 6(b), we plot the distribution or reported power-conversion efficiency (PCE) across cells and the materials are sorted by the highest reported PCE for a given material. The highest PCE is from delafossites $CuMO_2$ (M = Ga, Cr, Fe), spinel $NiCo_2O_4$, mixed anion compounds CuCSN and Cu_3PS_4, and binaries Cu_xO and CuI (with various doping schemes). We note that none of these p-type TC materials were first predicted computationally; to our knowledge, to date no predicted p-type TC has been used as a perovskite HTL. Additionally, these are results from laboratory-scale cells, not modules; none of the

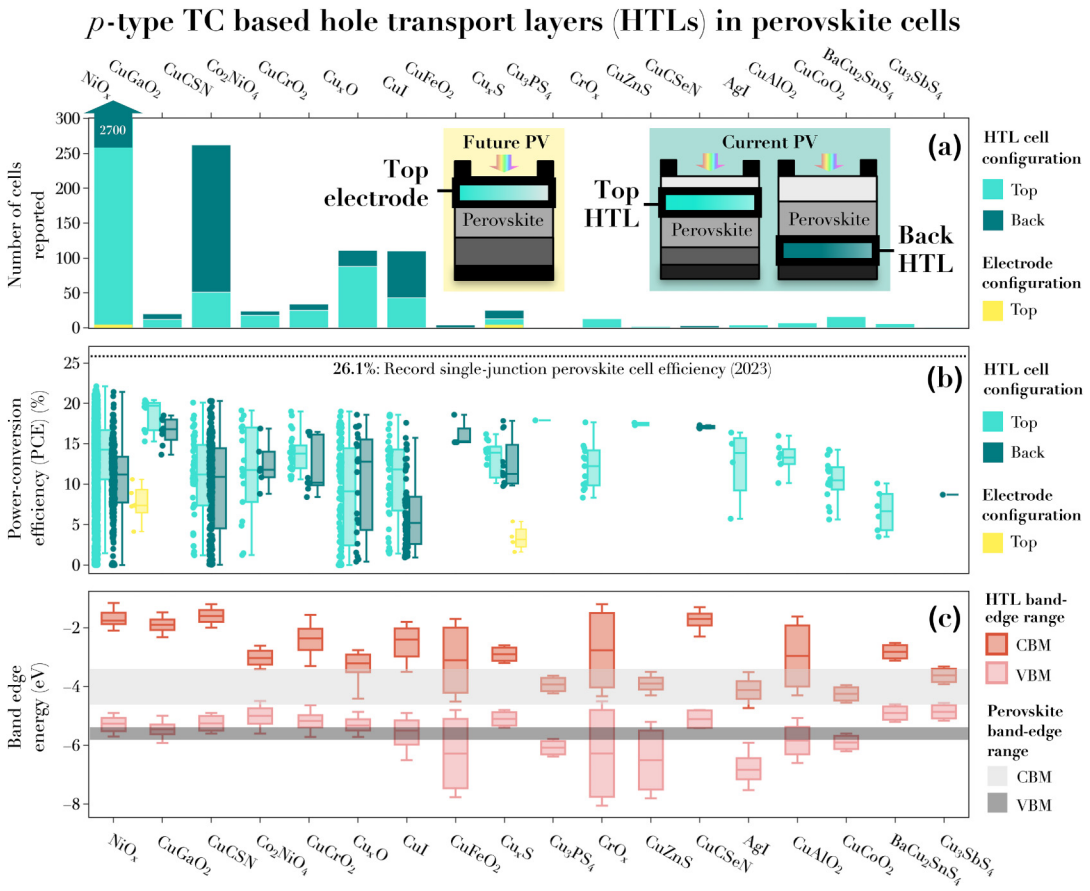

FIG. 6. A summary of various p-type TCs used as HTLs in laboratory-scale single-junction perovskite solar cells: (a) a histogram of the number of cells reported; (b) a box plot of the reported power-conversion efficiency (PCE); (c) the range of reported band edges from the literature. In (a) and (b), color refers to the cell configuration and whether the HTL is at the top or bottom of the cell (for details, see Fig. 2). The data sets to make this figure have been processed from the Perovskite Database [141] (containing studies from 2021 and earlier) and various literature reports and are available as a table and JUPYTER notebook in the Supplemental Material [34].

reported materials (except for NiO_x) have been reported in a large-area module.

A. Challenges at interfaces and junctions

Additional complexity emerges at device interfaces, where a TC is in contact with other material layers, which can lead to serious optimization challenges. Before incorporating into a full device, sometimes new contacts are tested on a heterojunction or a "half-cell" to assess the interface and demonstrate rectification properties (stage 6). One of the first challenges to emerge at the interface of a p-type TC and its adjacent layer(s) is interfacial stability. The interface must be stable without reacting, decomposing, or segregating into unintentional secondary materials or inducing trap states. For example, although $Cu_xZn_{1-x}S$ is stable as a thin film, growing it as a back contact to CdTe solar cells induces complete decomposition of the $Cu_xZn_{1-x}S$ layer into Cd-Zn-S and CuTe (see phase separation from electron microscopy in Fig. 5) [118]. Although NiO_x is commonly used as a HTM for perovskite solar cells, at certain processing conditions it has been shown to react with the perovskite layer and introduce an interfacial defect layer; similarly, NiO_x in contact with Si in a SHJ cell likely introduces an interfacial layer of SiO_x. The Materials Project's interfacial reaction calculator can be applied as a simple indicator of whether a reaction product is likely to form thermodynamically at an interface and, if so, the degree of instability (whether it will likely passivate or decompose). However even if an interface is thermodynamically stable, it can still degrade over time after operating in nonequilibrium conditions, such as in light-induced degradation (LID). For example, the morphology and doping of n-type top contacts can impact the degree of LID [142] and, in perovskites, HTMs and poly(3,4-ethylenedioxythiophene):poly(styrene-sulfonate) (PEDOT:PSS) degrade upon light exposure [143], but this effect is nontrivial to predict without experiments.

When incorporating a novel p-type layer into a PV device, electronic band edges have to be aligned such that they enable desired junction properties. Ideally, the valence

band maximum (VBM) of the p-type TC should be aligned to the VBM of the layer from which it extracts holes. In addition, the conduction band minimum (CBM) of the TC should be sufficiently shallow to form an electron-blocking barrier with the same layer. These criteria are important in particular for hole-selective contacts for thin-film PV devices and for p-type layers in tandems. For example, in CdTe solar cells, a rule of thumb is that the VBM offset of the p-type contact and CdTe absorber layer should be within 0.3 eV [144]. In Fig. 6(c), we plot literature-reported band offsets for p-type TCs used as HTLs in perovskite solar cells, showing that for most TCs, the VBM range is close to the range of various perovskite absorber layers (−5.42 eV to −5.77 eV, referenced to vacuum [145]). However, precise band alignment may not be crucial if the TC is placed next to another highly doped layer or if it is a tunneling layer. In SHJ cells, it has been shown that if the hole-selective contact is not highly doped, its VB has to be aligned very close to that of its neighboring layer (within approximately ±0.1 eV) to enable high efficiencies. On the contrary, if the p-type TC layer is highly doped above 10^{18} cm^3, high efficiency can be achieved within a wider tolerance to VB misalignment [51].

A combination of x-ray photoemission spectroscopy (XPS) and first-principles slab calculations can be used to assess band offsets of new TCs. Uncertainties of DFT alignments are less than ±0.3 eV with local-density approximation (LDA) and the generalized gradient approximation (GGA) Perdew-Burke-Ernzerhof (PBE) functional (this is included as error bars in Fig. 6) [146] and this error becomes problematic if a precise degree of alignment is required between layers. Band offsets can differ depending on the surface morphology, including the crystallographic plane, surface termination, and defects, so there is often a mismatch between computed bulk band offsets and measured offsets in polycrystalline TCs [147]. Band offsets are usually not computed early in TC screenings but sometimes are assessed in computational deep dives (stage 2). Offsets for an individual material are not sufficient to simulate band bending when in contact with another material, so continuum simulations should be also performed to assess band bending and quasi-Fermi-level splitting at a new interface.

In addition to chemical stability and electronic alignment, fabrication of the p-type TC layer must form strong bonds and mechanically adhere to adjacent layers. Mechanical breakage at interfaces and delamination can induce detrimental voids or pinholes, which can result in increased electrical resistance and heat losses, and air or moisture gaps can facilitate degradation. These challenges are exacerbated in layered anisotropic p-type TCs such as delafossite $CuAlO_2$, as highlighted in Fig. 5 for $CuAlO_2$-Si heterojunction diode devices [117], where high contact resistance due to poor adhesion has been a major barrier to scaling solar devices. It is expected that this may be the case for predicted layered structures such as $[Cu_2S_2][Ba_3Sc_2O_5]$ [148]. Some PV applications, such as perovskites, are moving toward flexible substrates, so designing p-type TCs layers to avoid mechanical breakages will become even more important as these devices come to market.

B. Practical solar cell design

When a solar cell is fabricated using a new contact material (stage 7), cell performance is determined not only by intrinsic material properties but also by interfacial properties—in particular, electronic band alignment—and the possible presence of interfacial defects. Surface passivation of contacts and absorbers is, in fact, an important line of research in thin-film and heterojunction-based PV devices; however, this topic goes beyond the purpose of this review [149,150]. Defects at interfaces can have different origins, from chemical intermixing to the presence of dangling bonds, among others. However, the role of these defects is rarely considered in early-stage materials design. Therefore, an open challenge is the development of screening metrics to assess interfacial or pinning defects that may arise at contact interfaces and how they may limit performance. To assess this, it is important to also predefine the type of absorber material and assess its properties simultaneously. Integrating methods that merge defect calculations and materials predictions with continuum interface simulations in solar cell contact layers could provide valuable insights into the behavior of device-relevant defects under actual operating conditions [151].

Besides engineering defects, another important consideration for device design is optimizing the fabrication method, including designing for temperature stability (most devices have a "thermal budget"). A growth method that works well for synthesizing a single film on a substrate may not be appropriate for a full device stack. In thin-film solar cells, contact layers with low thermal budgets of a few hundred degrees Celsius are usually preferable; the process temperature of the TC should not be so high as to cause unwanted reactions in the bulk of the absorber or at the interface. However, many of the synthesis recipes for the best reported p-type TCs involve high temperatures during some step of the process [103]. For example, Mg-doped $CuCrO_2$ grown by sputtering is one of the highest-performing p-type TCs but requires a synthesis temperature of 750 °C, which limits its practicality for devices [3]. However, recent developments have enabled low-temperature $CuCrO_2$ synthesis and incorporation at an HTL in perovskite cells with high efficiency (see Fig. 6) [152]. Furthermore, plasma-assisted techniques such as sputtering, pulsed laser deposition (PLD), and plasma-enhanced chemical vapor deposition (PECVD) are often used to deposit TCs and these methods can be harsh on the underlying material; however, it has recently been shown

that oxide TCs can be deposited on perovskites with very low damage by PLD [153,154]. P-type TC films for PV applications that will operate in the sun also need to be stable under UV irradiation, both in their bulk form and at their interfaces, though this is less important in superstrate devices, in which glass absorbs much of the UV. It is also important to consider the lifetime of the device when designing materials to be incorporated; e.g., whether migration of dopants or segregation into secondary phases will occur over time.

In PV contacts, the tolerance to nonideal properties such as electronic misalignment depends strongly on the device architecture. The tolerances of a TC property within a given device may depend on multiple material and junction properties and therefore may be better described by a multiobjective optimization scheme rather than a serial-screening "funnel." For example, precise band alignment may not be as relevant if the TC is placed next to another highly doped layer or if it is a tunneling layer. In SHJ cells, it has been shown that if the hole-selective contact is not highly doped, its VB has to be aligned very close to that of its neighboring layer (within approximately ± 0.1 eV) to enable high efficiencies. However, if the p-type TC layer is highly doped above 10^{18} cm^3, high efficiency can be achieved within a wider tolerance to VB misalignment [51]. Other properties besides alignment also depend on the device configuration. Perhaps most trivially, the wavelengths to which a material must be transparent depend on the absorption spectrum of the absorber layer. Similarly, the high mobility requirement and threshold varies dramatically across absorber technologies and device designs.

Similar to the novelty bias mentioned previously, one practical challenge when incorporating new materials into solar cell devices is that device architectures are optimized around conventional materials. For example, SHJ solar cells have been highly optimized using a hydrogenated boron-doped amorphous silicon (B-doped p-type a-Si:H) and ITO bilayer as the hole-selective top contact, with thicknesses and dopings of these layers and adjacent layers tuned specifically to work well with these materials. Thus, one cannot simply remove a highly optimized material (e.g., a-Si), insert a new layer (e.g., a novel p-type TC) into the same device stack, and expect it to deliver optimal properties, even if that new material has high transparency and conductivity. Rather, the entire device may have to be reoptimized to accommodate the new architecture, energetic alignment, and emergent defects from inserting this new layer. However, this can be tedious when working with a large quantity of candidates in high-throughput methods and thus this is not typically done. As a result, a feedback loop ensues: device layers are limited to a small set of materials (i.e., small compared to the size of computational databases) that are well optimized, heavily characterized, easy and cheap to grow, and therefore are more likely to work well in a given device architecture. Then, more resources are invested in further optimizing these already well-optimized materials and new materials such as predicted p-type TCs have a larger barrier to entry.

C. Scalability and sustainability

To our knowledge, a high-performance solar module using p-type TC contacts has not yet been fabricated. However, if a high-performance p-type TC can someday be successfully integrated into a small-scale laboratory cell, the next stage toward commercialization would involve scaling up to full-sized module devices (stage 9 in Fig. 3), which would introduce a new set of challenges. Module performance tends to lag behind cell performance, namely, due to the requirement for larger-surface-area deposition and lower tolerance for nonuniformities [155]. Challenges such as large-area conformity, uniform crystallinity, and strong adhesion without pinholes are exacerbated for thinner films [156] and since contact layers tend to be thinner than absorber layers in solar cells, there is likely less tolerance in contacts for such nonidealities. TC layers in modules also need to be stable for decades and maintain high transparency and electrical conductivity while minimizing resistance losses and avoiding localized performance drops due to defects.

Several deposition methods used regularly to synthesize TCs in laboratory-based devices are nonuniform by design and challenging to scale, such as spin coating and PLD, though wafer-scale PLD of ITO, Zr:In_2O_3, and SnO_2 for perovskites or SHJ cells has recently been demonstrated [154,157,158]. Other deposition methods such as sputtering are regularly adapted for large-area deposition but require reoptimization and often result in performance lower than that of small cells. ITO is usually deposited by large-area sputtering in SHJ, perovskite, and SHJ-perovskite tandem modules [159], while in CdTe modules, the n-type top-contact FTO is usually deposited by CVD and can be done by the glass manufacturer [160]. Several studies have demonstrated large-area fabrication of buffers and contacts such as NiO_x for perovskite module applications [161]. However, scaling CuI while maintaining good performance remains an open challenge toward commercialization, largely due to instabilities from moisture, oxygen, and elevated temperatures [162] (see the degraded 6-month-aged sample in Fig. 5 [119]) and similar challenges apply to other inorganic HTLs. Even if physically possible to scale, many high-vacuum synthesis techniques such as MBE are simply too expensive and labor-intensive to use commercially. Developing low-cost module-scale synthesis techniques such as roll-to-roll printing early on in the p-type TC "design-to-device" development process could enable more rapid integration into next-generation modules. Incorporating economic

modeling such as techno-economic analysis can help guide integration of new materials into low-cost devices [163].

Interdisciplinary collaborations between academia, national laboratories, and industry could help address scaling challenges. Researchers might assess the effects of large areas and conformity on the properties of early-stage TCs, whether low-cost scalable deposition processes are suitable for a given TC, and how film quality trades off with cost and scalability when moving from epitaxial or single-crystal films to polycrystalline or amorphous films (realistic for large-scale processing). National laboratories such as NREL could set up testing and standardization protocols for large-scale TCs, and platforms to share data. Although thin-film PV companies have likely explored emerging p-type TCs without publishing, successful public-private partnerships (e.g., First Solar's p-type back-contact research collaborations [164,165]) demonstrate the potential for joint efforts to advance module development. Continued collaboration could accelerate commercial scaling of TCs by linking the critical needs of industry with the capabilities and limitations of basic research.

Although the ultimate goal of scaling solar photovoltaics is to mitigate climate change, input and outputs from production and deployment may cause unintentional consequences such as damage to ecosystems and human health and there is an ethical responsibility to minimize harm as we scale new materials such as TCs [166,167]. Techniques such as life-cycle assessment (LCA) can be used to identify key sources of negative impacts within the life cycle of a technology and guide research directions to reduce harm [168]. PV devices have much lower environmental impacts than fossil-fuel technologies due to negligible inputs and outputs during operation but impacts do emerge from mining, refining, manufacturing, and decommissioning [169]. Mining of critical PV materials can lead to resource depletion, human-health impacts, and ecotoxicity, and has motivated shifting toward "Earth-abundant" materials [170], such as moving away from indium in n-type TCs. However, in all PV devices, most life-cycle greenhouse-gas (GHG) emissions are from the energy intensity of material production rather than mining [171]. In conventional PV systems, emissions are primarily from refining solar-grade silicon; but in emerging PV applications, many of these manufacturing-stage emissions are also from contact layers. For example, in perovskite tandems, fabrication of contacts and buffers such as Spiro-MeOTAD and sputtered ITO contribute significantly to GHG emissions from the cell [159]. Thin-film PV modules tend to yield lower impacts compared to Si-based modules [172,173], which motivates scaling thin-film PV devices with high-performing heterojunction contacts, so designing contact materials with low-energy-intensity processing could significantly reduce life-cycle impacts.

Historically, LCAs are conducted after technologies reach commercial scale, which can lead to "technology lock-in" that makes it challenging to replace harmful materials [167]. While there have been instances of course correction and phase out—e.g., recent efforts to reduce Co content in lithium ion batteries to address supply chain hazards by replacing $LiCoO_2$ cathodes with $LiNi_xMn_yCo_{1-x-y}O_2$ (NMC) (which still rely on lithium and nickel) [174]—some of this lock-in is unavoidable if we want to rapidly deploy renewable energy. One such trade-off is that delaying deployment to wait for PV systems with lower embodied carbon would result in more emissions than installing existing PV modules, so it is important that conventional Si (e.g., PERC) is rapidly installed [175].

Low-TRL emerging PV technologies are years or even decades away from commercialization but offer serious opportunities for sustainability improvements. These are technologies in which TCs play an important role, so designing new contacts for emerging PV applications with low environmental impacts could make a big impact. Assessing impacts early in the materials design phase is challenging [176], particularly when the synthesis route is unknown, and especially for p-type TCs, since an understanding of their underlying physics and design criteria is still lacking. Computational materials discovery often assumes that optimization can reduce impacts, e.g., from replacement of elements or reduction of processing energy. For example, a computationally predicted p-type TC ($BeSiP_2$) has recently been proposed using the new design metric of forbidden optical transitions. Although this particular material contains Be and is impractical to scale, but this design metric may be applicable to an Earth-abundant version that has not yet been discovered [30]; being too restrictive, at early stages could lead to missed opportunities. However, we should keep in mind that there is always a certain amount of risk with this approach, since later-stage replacements can be difficult. For example, despite significant research efforts, replacing a toxic element in perovskite absorbers (Pb) with a nontoxic element (e.g., Sn or Bi) has not yet yielded high enough performance [177].

The following question arises: how can materials scientists integrate life-cycle thinking throughout the full process of materials discovery and design to prevent "locking-in" technologies with detrimental impacts? This challenge calls for the development of early-stage metrics and strategies for embedding sustainability early in the materials design process, such as accounting for material criticality, embodied carbon, or social impacts from mining and refining in elemental precursors, or estimating possible energy consumption during manufacturing [176]. Inspiration can be drawn from recent approaches such as Emerging Materials Risk Analysis [178], "upscaling" manufacturing assessments [179], and the framework of anticipatory

LCA [167,180], as well as the development of open-source open-access LCA infrastructure such as the BRIGHTWAY framework, which can connect with materials discovery infrastructure [181]. Moreover, we encourage the continued development of new metrics—assessing for embedded carbon, coproduct assessment, manufacturing impacts, and end-of-life considerations—that can be incorporated into the design of p-type TCs for emerging PV applications and the discovery of sustainable materials in general.

V. INSIGHTS FOR FUTURE DESIGN OF p-TYPE TCs

This paper has reviewed various disconnects throughout the materials discovery process of p-type TCs, spanning from computational design to material synthesis and from laboratory-scale devices to scalable sustainable modules. We have compiled and made available an extensive set of literature data tables to help researchers identify and explore such disconnects [34]. To address these disconnects to design commercially relevant p-type transparent conductors, we propose the following recommendations for materials designers:

(1) *Improve and benchmark descriptors for p-type TCs, especially for band gap, dopability, and mobility*. Since the first high-throughput screening for p-type TCOs appeared a decade ago, first-principles computational methods have improved tremendously and computing power has increased. More accurate assessment of band gap and mobility are emerging with different levels of accuracy and cost. Assessment of defects and dopability is still among the most expensive computations to perform but they have been automatized and tractable high-throughput defect approaches are emerging. Predictive low-cost descriptors of dopability have not yet been developed and the inclusion of transport properties such as grain-boundary scattering at early stages is not common, but both of these pursuits would accelerate screening tremendously. In the past decade, the available data sets from which to screen have also grown tremendously, such as in the Materials Project and other large databases, and opportunities to use ML to speed up the screening process are naturally emerging from these data sets.

(2) *Judiciously assess whether predictions are actually synthesizable*. Before laboratory-based synthesis, higher-accuracy metrics should be used to assess the synthesizability of emerging screening candidates. To closer approximate synthesizability of realistic thin films and interfaces, computational screenings should seek better metrics than E_{hull} alone. The ability to move from thermodynamic metrics to assessment of synthesizability in screenings is an important future frontier of computational materials design.

(3) *Establish standards and a consensus on how defect calculations are run and interpreted*. There are inconsistencies across the literature in terms of which corrections to use and qualitative interpretation of formation energies and Fermi-level pinning. To avoid inconsistencies and assist comparison across the literature, quantitative assessment of carrier concentration is recommended rather than simply stating whether a material is "dopable." Following lessons learned from the quadruple perovskite study of Hu *et al.* about the "importance of reasonable band gap description and chemical boundary determination in predicting defect thermodynamics" [96], it is recommended to standardize running hybrid defect calculations to confirm p-type dopability.

(4) *Screen for tunability and tolerance ranges, rather than a single compound with a single property*. Tuning stoichiometry and doping in the laboratory can introduce effects not typically considered in bulk calculations, so techniques to simulate tunability would be useful. While very important in practical materials, the effects of alloying and off-stoichiometry are not often not taken into account early on in high-throughput studies, so addressing this gap could lead to new TCs and other material predictions. Automated experiments, though not yet used in p-type TC discovery as far as we know, are a promising future direction to incorporate tunability by linking feedback loops of experimental synthesis and characterization to ML and computational data. This could enable rapid exploration of chemical potential space and stoichiometry to limit false positives and identify nonlinearities.

(5) *Be judicious whether metrics and materials are device appropriate*. Searches should be tailored to specific applications, rather than a generic "high-performance" p-type TC. Some properties matter less than others depending on application and by using generic screenings, useful targeted materials may be overlooked. For example, for some devices there may be trade-offs between properties such that achieving optimal performance is a multiparameter optimization problem (e.g., carrier concentration and band alignment can be coupled). Assessing these trade-offs may require iterative research and learning between stages 1 and 9 in Fig. 3 and synergizing high-throughput computation with multiscale modeling and device testing.

(6) *Develop sustainability and scalability metrics to incorporate early in the materials design process*. To avoid "locking-in" technologies with detrimental environmental effects, materials scientists

should integrate life-cycle thinking throughout the design process, drawing inspiration from recent methodologies such as Emerging Materials Risk Analysis and anticipatory life-cycle assessment. The development of early-stage metrics assessing embedded carbon, co-product impacts, manufacturing impacts, and end-of-life aspects could help guide sustainable-materials discovery in the field of emerging photovoltaics and beyond.

(7) *Conduct more interdisciplinary analyses to bring computed materials into devices.* Historically, separate research teams have performed computations, synthesis, fabrication, and scale-up modeling, which can lead to communication barriers. However, there is a recent trend toward connecting theorists, experimentalists, and analysts on a single project. Ultimately, more communication and collaboration between scientists across various stages of materials discovery and various stages of technology readiness can help address these disconnects and lead to more effective design.

The goal of materials discovery is to predict a new material from first principles that can ultimately scale up and be used in devices such as solar panels for more efficient and sustainable technological development. Although we have made major progress in the field of predicting p-type TCs and scaling into photovoltaic devices, there is still a large gap between the research stage of proposing a new candidate and actually incorporating the candidate into a device. In this perspective, we have highlighted some major disconnects from the past ten years of research into p-type TCs, as well as insights to guide new research into designing, synthesizing, and scaling materials. We hope that these insights, applied not only to future design of p-type TCs but toward materials design in general, can help catalyze more targeted and rapid discovery of materials to advance sustainable energy technologies.

ACKNOWLEDGMENTS

This work was supported by the U.S. Department of Energy, Office of Science, Basic Energy Sciences under Contract No. DE-AC02-05-CH11231 (Materials Project program KC23MP). R.W.R. was supported by the University of California, Berkeley Chancellor's Fellowship and the National Science Foundation (NSF) Graduate Research Fellowship under Grants No. DGE1106400 and No. DGE175814. R.W.-R. also acknowledges financial support from a Distinguished Postdoctoral Fellowship at the University of Washington Clean Energy Institute. G.H. acknowledges support from the U.S. Department of Energy, Office of Science, Basic Energy Sciences under Award No. DE-SC0023509. The work of A.C. was supported in part by a research grant (42140) from VILLUM FONDEN and co-funded by the European Union (ERC, IDOL, 101040153).

We highlight the author contributions to this study using the CRediT taxonomy. R.W.R.: Conceptualization, Methodology, Data Curation, Visualization, Investigation, Writing—Original Draft, Writing—Review & Editing, Funding Acquisition, Project Administration; M.M.M.: Methodology, Investigation, Writing—Review & Editing, Funding Acquisition; G.H.: Methodology, Investigation, Writing—Review & Editing, Funding Acquisition; A.C.: Methodology, Investigation, Writing—Review & Editing, Funding Acquisition.

Views and opinions expressed are however those of the authors only and do not necessarily reflect those of the European Union or the European Research Council. Neither the European Union nor the granting authority can be held responsible for them.

[1] D. S. Ginley and J. D. Perkins*Transparent Conductors* (Springer, New York, 2011).

[2] J. Willis and D. O. Scanlon, Latest directions in p-type transparent conductor design, J. Mater. Chem. C **9**, 11995 (2021).

[3] R. Nagarajan, A. Draeseke, A. Sleight, and J. Tate, p-type conductivity in $CuCr_{1-x}Mg_xO_2$ films and powders, J. Appl. Phys. **89**, 8022 (2001).

[4] J. Wang, J. Li, and S.-S. Li, Native p-type transparent conductive CuI via intrinsic defects, J. Appl. Phys. **110**, 054907 (2011).

[5] A. E. Delahoy and S. Y. Guo, Transparent and semitransparent conducting film deposition by reactive-environment, hollow cathode sputtering, J. Vac. Sci. Technol., A **23**, 1215 (2005).

[6] A. Jain, S. P. Ong, G. Hautier, W. Chen, W. D. Richards, S. Dacek, S. Cholia, D. Gunter, D. Skinner, G. Ceder, and K. A. Persson, Commentary: The Materials Project: A materials genome approach to accelerating materials innovation, APL Mater. **1**, 011002 (2013).

[7] S. Curtarolo, W. Setyawan, S. Wang, J. Xue, K. Yang, R. H. Taylor, L. J. Nelson, G. L. W. Hart, S. Sanvito, M. Buongiorno-Nardelli, N. Mingo, and O. Levy, AFLOWLIB.ORG: A distributed materials properties repository from high-throughput *ab initio* calculations, Comput. Mater. Sci. **58**, 227 (2012).

[8] S. Kirklin, J. E. Saal, B. Meredig, A. Thompson, J. W. Doak, M. Aykol, S. Rühl, and C. Wolverton, The open quantum materials database (OQMD): Assessing the accuracy of DFT formation energies, npj Comput. Mater. **1**, 15010 (2015).

[9] G. Brunin, G.-M. Rignanese, and G. Hautier, High-performance transparent conducting oxides through small-polaron transport, Phys. Rev. Mater. **3**, 064602 (2019).

[10] G. Hautier, A. Miglio, G. Ceder, G.-M. Rignanese, and X. Gonze, Identification and design principles of low hole effective mass p-type transparent conducting oxides, Nat. Commun. **4**, 2292 (2013).

[11] J. B. Varley, A. Miglio, V. A. Ha, M. J. V. Setten, G. M. Rignanese, and G. Hautier, High-throughput design of non-oxide p-type transparent conducting materials: Data mining, search strategy, and identification of boron phosphide, Chem. Mater. **29**, 2568 (2017).

[12] R. Woods-Robinson, D. Broberg, A. Faghaninia, A. Jain, S. S. Dwaraknath, and K. A. Persson, Assessing high-throughput descriptors for prediction of transparent conductors, Chem. Mater. **30**, 8375 (2018).

[13] G. Brunin, F. Ricci, V.-A. Ha, G.-M. Rignanese, and G. Hautier, Transparent conducting materials discovery using high-throughput computing, npj Comput. Mater. **5**, 63 (2019).

[14] H. Peng, A. Zakutayev, S. Lany, T. R. Paudel, M. d'Avezac, P. F. Ndione, J. D. Perkins, D. S. Ginley, A. R. Nagaraja, N. H. Perry, T. O. Mason, and A. Zunger, Li-doped Cr_2MnO_4: A new p-type transparent conducting oxide by computational materials design, Adv. Funct. Mater. **23**, 5267 (2013).

[15] A. Bhatia, G. Hautier, T. Nilgianskul, A. Miglio, J. Sun, H. J. Kim, K. H. Kim, S. Chen, G.-M. Rignanese, X. Gonze, and J. Suntivich, High-mobility bismuth-based transparent p-type oxide from high-throughput material screening, Chem. Mater. **28**, 30 (2015).

[16] N. Sarmadian, R. Saniz, B. Partoens, and D. Lamoen, Easily doped p-type, low hole effective mass, transparent oxides, Sci. Rep. **6**, 20446 (2016).

[17] B. A. D. Williamson, J. Buckeridge, J. Brown, S. Ansbro, R. G. Palgrave, and D. O. Scanlon, Engineering valence band dispersion for high mobility p-type semiconductors, Chem. Mater. **29**, 2402 (2016).

[18] J. Shi, T. F. Cerqueira, W. Cui, F. Nogueira, S. Botti, and M. A. Marques, High-throughput search of ternary chalcogenides for p-type transparent electrodes, Sci. Rep. **7**, 43179 (2017).

[19] R. K. M. Raghupathy, T. D. Kühne, C. Felser, and H. Mirhosseini, Rational design of transparent p-type conducting non-oxide materials from high-throughput calculations, J. Mater. Chem. C **6**, 541 (2018).

[20] R. Kormath Madam Raghupathy, H. Wiebeler, T. D. Kuhne, C. Felser, and H. Mirhosseini, Database screening of ternary chalcogenides for p-type transparent conductors, Chem. Mater. **30**, 6794 (2018).

[21] K. Yim, Y. Youn, M. Lee, D. Yoo, J. Lee, S. H. Cho, and S. Han, Computational discovery of p-type transparent oxide semiconductors using hydrogen descriptor, npj Comput. Mater. **4**, 17 (2018).

[22] Y. Youn, M. Lee, D. Kim, J. K. Jeong, Y. Kang, and S. Han, Large-scale computational identification of p-type oxide semiconductors by hierarchical screening, Chem. Mater. **31**, 5475 (2019).

[23] V.-A. Ha, G. Yu, F. Ricci, D. Dahliah, M. J. van Setten, M. Giantomassi, G.-M. Rignanese, and G. Hautier, Computationally driven high-throughput identification of CaTe and Li_3Sb as promising candidates for high-mobility p-type transparent conducting materials, Phys. Rev. Mater. **3**, 034601 (2019).

[24] Y. Hu, X. Yao, D. G. Schlom, S. Datta, and K. Cho, First principles design of high hole mobility p-type Sn–O–X ternary oxides: Valence orbital engineering of Sn^{2+} in Sn^{2+}–O–X by selection of appropriate elements X, Chem. Mater. **33**, 212 (2020).

[25] J. Shi, E. A. Rubinstein, W. Li, J. Zhang, Y. Yang, T.-L. Lee, C. Qin, P. Yan, J. L. MacManus-Driscoll, D. O. Scanlon, and K. H. Zhang, Modulation of the Bi^{3+} $6s^2$ lone pair state in perovskites for high-mobility p-type oxide semiconductors, Adv. Sci. **9**, 2104141 (2022).

[26] F. Yan, X. Zhang, Y. G. Yu, L. Yu, A. Nagaraja, T. O. Mason, and A. Zunger, Design and discovery of a novel half-Heusler transparent hole conductor made of all-metallic heavy elements, Nat. Commun. **6**, 7308 (2015).

[27] V.-A. Ha, B. Karasulu, R. Maezono, G. Brunin, J. B. Varley, G.-M. Rignanese, B. Monserrat, and G. Hautier, Boron phosphide as a p-type transparent conductor: Optical absorption and transport through electron-phonon coupling, Phys. Rev. Mater. **4**, 065401 (2020).

[28] A. Crovetto, J. M. Adamczyk, R. R. Schnepf, C. L. Perkins, H. Hempel, S. R. Bauers, E. S. Toberer, A. C. Tamboli, T. Unold, and A. Zakutayev, Boron phosphide films by reactive sputtering: Searching for a p-type transparent conductor, Adv. Mater. Interfaces **9**, 2200031 (2022).

[29] M. Barone, M. Foody, Y. Hu, J. Sun, B. Frye, S. S. Perera, B. Subedi, H. Paik, J. Hollin, M. Jeong, K. Lee, C. H. Winter, N. J. Podraza, K. Cho, A. Hock, and D. G. Schlom, Growth of Ta_2SnO_6 films, a candidate wide-band-gap p-type oxide, J. Phys. Chem. C **126**, 3764 (2022).

[30] R. Woods-Robinson, Y. Xiong, J.-X. Shen, N. Winner, M. K. Horton, M. Asta, A. M. Ganose, G. Hautier, and K. A. Persson, Designing transparent conductors using forbidden optical transitions, Matter **6**, 3021 (2023).

[31] G. Hautier, A. Miglio, D. Waroquiers, G.-M. Rignanese, and X. Gonze, How does chemistry influence electron effective mass in oxides? A high-throughput computational analysis, Chem. Mater. **26**, 5447 (2014).

[32] A. J. Jackson, B. J. Parrett, J. Willis, A. M. Ganose, W. W. W. Leung, Y. Liu, B. A. D. Williamson, T. K. Kim, M. Hoesch, L. S. I. Veiga, R. Kalra, J. Neu, C. A. Schmuttenmaer, T.-L. Lee, A. Regoutz, T.-C. Lee, T. D. Veal, R. G. Palgrave, R. Perry, and D. O. Scanlon, Computational prediction and experimental realization of Earth-abundant transparent conducting oxide Ga-doped $ZnSb_2O_6$, ACS Energy Lett. **7**, 3807 (2022).

[33] V. Deutscher Maschinenbau-Anstalten (VDMA), International technology roadmap for photovoltaic (ITRPV), Tech. Rep., ITRPV, 2024.

[34] See the Supplemental Material at http://link.aps.org/supplemental/10.1103/PRXEnergy.3.031001 for a Supplemental Material PDF, a corresponding table (with computational predictions, experimental reports, literature reviews, band offsets, and perovskite solar cells with p-type TCs), and JUPYTER notebooks to generate figures.

[35] B. J. Stanbery, M. Woodhouse, and J. van de Lagemaat, Photovoltaic deployment scenarios toward global decarbonization: Role of disruptive technologies, Solar RRL **7**, 2300102 (2023).

[36] D. Dahliah, G. Brunin, J. George, V.-A. Ha, G.-M. Rignanese, and G. Hautier, High-throughput computational search for high carrier lifetime, defect-tolerant solar absorbers, Energy Environ. Sci. **14**, 5057 (2021).

[37] D. Broberg, K. Bystrom, S. Srivastava, D. Dahliah, B. A. D. Williamson, L. Weston, D. O. Scanlon, G.-M. Rignanese, S. Dwaraknath, J. Varley, K. A. Persson, M. Asta, and G. Hautier, High-throughput calculations of charged point defect properties with semi-local density functional theory—performance benchmarks for materials screening applications, npj Comput. Mater. **9**, 72 (2023).

[38] A. N. Fioretti and M. Morales-Masis, Bridging the *p*-type transparent conductive materials gap: Synthesis approaches for disperse valence band materials, J. Photonics Energy **10**, 042002 (2020).

[39] T. Minemoto, T. Matsui, H. Takakura, Y. Hamakawa, T. Negami, Y. Hashimoto, T. Uenoyama, and M. Kitagawa, Theoretical analysis of the effect of conduction band offset of window/CIS layers on performance of CIS solar cells using device simulation, Sol. Energy Mater. Sol. Cells **67**, 83 (2001).

[40] NREL, Best Research-Cell Efficiency Chart, https://www.nrel.gov/pv/cell-efficiency.html, 2023 (Accessed: 2023-11-07).

[41] NREL, Champion Photovoltaic Module Efficiency Chart, https://www.nrel.gov/pv/module-efficiency.html, 2023 (Accessed: 2023-11-07).

[42] D. Fraser and H. Cook, Highly conductive, transparent films of sputtered $In_{2-x}Sn_xO_{3-y}$, J. Electrochem. Soc. **119**, 1368 (1972).

[43] G. Haacke, New figure of merit for transparent conductors, J. Appl. Phys. **47**, 4086 (1976).

[44] R. G. Gordon, Criteria for choosing transparent conductors, MRS Bull. **25**, 52 (2000).

[45] I. Cisneros-Contreras, A. Muñoz-Rosas, and A. Rodríguez-Gómez, Resolution improvement in Haacke's figure of merit for transparent conductive films, Results Phys. **15**, 102695 (2019).

[46] K. H. Zhang, K. Xi, M. G. Blamire, and R. G. Egdell, *P*-type transparent conducting oxides, J. Phys.: Condens. Matter **28**, 383002 (2016).

[47] A. S. Mirza, M. Pols, W. Soltanpoor, S. Tao, G. Brocks, and M. Morales-Masis, The role of sulfur in sulfur-doped copper (i) iodide *p*-type transparent conductors, Matter **6**, 4306 (2023).

[48] F. Geng, Y.-N. Wu, D. Splith, L. Wang, X. Kang, X. Chen, P. Guo, S. Liang, L. Yang, M. Lorenz, M. Grundmann, J. Zhu, and C. Yang, Amorphous transparent Cu(S,I) thin films with very high hole conductivity, J. Phys. Chem. Lett. **14**, 6163 (2023).

[49] X. Zhang, L. Zhang, J. D. Perkins, and A. Zunger, Intrinsic transparent conductors without doping, Phys. Rev. Lett. **115**, 176602 (2015).

[50] K. Lejaeghere, S. Cottenier, and V. Van Speybroeck, Ranking the stars: A refined pareto approach to computational materials design, Phys. Rev. Lett. **111**, 075501 (2013).

[51] R. Woods-Robinson, V. Stevanović, S. Lany, K. N. Heinselman, M. K. Horton, K. A. Persson, and A. Zakutayev, Role of disorder in the synthesis of metastable zinc zirconium nitrides, Phys. Rev. Mater. **6**, 043804 (2022).

[52] R. Gautier, X. Zhang, L. Hu, L. Yu, Y. Lin, T. O. Sunde, D. Chon, K. R. Poeppelmeier, and A. Zunger, Prediction and accelerated laboratory discovery of previously unknown 18-electron ABX compounds, Nat. Chem. **7**, 308 (2015).

[53] J. Xu, J.-B. Liu, J. Wang, B.-X. Liu, and B. Huang, Prediction of novel *p*-type transparent conductors in layered double perovskites: A first-principles study, Adv. Funct. Mater. **28**, 1800332 (2018).

[54] W. Sun, S. T. Dacek, S. P. Ong, G. Hautier, A. Jain, W. D. Richards, A. C. Gamst, K. A. Persson, and G. Ceder, The thermodynamic scale of inorganic crystalline metastability, Sci. Adv. **2**, e1600225 (2016).

[55] M. Aykol, S. S. Dwaraknath, W. Sun, and K. A. Persson, Thermodynamic limit for synthesis of metastable inorganic materials, Sci. Adv. **4**, eaaq0148 (2018).

[56] V. I. Hegde, M. Aykol, S. Kirklin, and C. Wolverton, The phase stability network of all inorganic materials, Sci. Adv. **6**, eaay5606 (2020).

[57] C. J. Bartel, S. L. Millican, A. M. Deml, J. R. Rumptz, W. Tumas, A. W. Weimer, S. Lany, V. Stevanović, C. B. Musgrave, and A. M. Holder, Physical descriptor for the Gibbs energy of inorganic crystalline solids and temperature-dependent materials chemistry, Nat. Commun. **9**, 4168 (2018).

[58] V. Stevanović, Sampling polymorphs of ionic solids using random superlattices, Phys. Rev. Lett. **116**, 075503 (2016).

[59] S. Haastrup, M. Strange, M. Pandey, T. Deilmann, P. S. Schmidt, N. F. Hinsche, M. N. Gjerding, D. Torelli, P. M. Larsen, A. C. Riis-Jensen, J. Gath, K. W. Jacobsen, J. J. Mortensen, T. Olsen, and K. S. Thygesen, The computational 2D materials database: High-throughput modeling and discovery of atomically thin crystals, 2D Materials **5**, 042002 (2018).

[60] M. Aykol, J. H. Montoya, and J. Hummelshøj, Rational solid-state synthesis routes for inorganic materials, J. Am. Chem. Soc. **143**, 9244 (2021).

[61] N. J. Szymanski, Y. Zeng, H. Huo, C. J. Bartel, H. Kim, and G. Ceder, Toward autonomous design and synthesis of novel inorganic materials, Mater. Horiz. **8**, 2169 (2021).

[62] A. Davariashtiyani, Z. Kadkhodaie, and S. Kadkhodaei, Predicting synthesizability of crystalline materials via deep learning, Commun. Mater. **2**, 115 (2021).

[63] H. Huo, C. J. Bartel, T. He, A. Trewartha, A. Dunn, B. Ouyang, A. Jain, and G. Ceder, Machine-learning rationalization and prediction of solid-state synthesis conditions, Chem. Mater. **34**, 7323 (2022).

[64] N. J. Szymanski, B. Rendy, Y. Fei, R. E. Kumar, T. He, D. Milsted, M. J. McDermott, M. Gallant, E. D. Cubuk, A. Merchant, H. Kim, A. Jain, C. J. Bartel, K. Persson, Y. Zeng, and G. Ceder, An autonomous laboratory for the accelerated synthesis of novel materials, Nature **624**, 86 (2023).

[65] J. H. Montoya, C. Grimley, M. Aykol, C. Ophus, H. Sternlicht, B. H. Savitzky, A. M. Minor, S. B. Torrisi, J. Goedjen, C.-C. Chung, A. H. C. Comstock, and S. Sun, How the AI-assisted discovery and synthesis of a ternary oxide highlights capability gaps in materials science, Chem. Sci. **15**, 5660 (2024).

[66] M. J. McDermott, S. S. Dwaraknath, and K. A. Persson, A graph-based network for predicting chemical reaction pathways in solid-state materials synthesis, Nat. Commun. **12**, 3097 (2021).

[67] M. J. McDermott, B. C. McBride, C. E. Regier, G. T. Tran, Y. Chen, A. A. Corrao, M. C. Gallant, G. E. Kamm,

C. J. Bartel, K. W. Chapman, P. G. Khalifah, G. Ceder, J. R. Neilson, and K. A. Persson, Assessing thermodynamic selectivity of solid-state reactions for the predictive synthesis of inorganic materials, ACS Cent. Sci. **9**, 1957 (2023).

[68] J. Yano, K. J. Gaffney, J. Gregoire, L. Hung, A. Ourmazd, J. Schrier, J. A. Sethian, and F. M. Toma, The case for data science in experimental chemistry: Examples and recommendations, Nat. Rev. Chem. **6**, 357 (2022).

[69] J. M. Gregoire, L. Zhou, and J. A. Haber, Combinatorial synthesis for AI-driven materials discovery, Nat. Synthesis **2**, 493 (2023).

[70] C. Toher, C. Oses, D. Hicks, and S. Curtarolo, Unavoidable disorder and entropy in multi-component systems, npj Comput. Mater. **5**, 69 (2019).

[71] A. Walsh and J.-S. Park, The holey grail of transparent electronics, Matter **3**, 604 (2020).

[72] H. Kawazoe, M. Yasukawa, H. Hyodo, M. Kurita, H. Yanagi, and H. Hosono, *P*-type electrical conduction in transparent thin films of $CuAlO_2$, Nature **389**, 939 (1997).

[73] K. Ahn, G. H. Kim, S.-J. Kim, J. Kim, G.-S. Ryu, P. Lee, B. Ryu, J. Y. Cho, Y.-H. Kim, J. Kang, H. Kim, Y.-Y. Noh, and M.-G. Kim, Highly conductive p-type transparent conducting electrode with sulfur-doped copper iodide, Chem. Mater. **34**, 10517 (2022).

[74] M. Kumar, A. Dubey, N. Adhikari, S. Venkatesan, and Q. Qiao, Strategic review of secondary phases, defects and defect-complexes in kesterite CZTS-Se solar cells, Energy Environ. Sci. **8**, 3134 (2015).

[75] L. Y. Liang, Z. M. Liu, H. T. Cao, Y. Y. Shi, X. L. Sun, Z. Yu, A. H. Chen, H. Z. Zhang, and Y. Q. Fang, Improvement of phase stability and accurate determination of optical constants of SnO thin films by using Al_2O_3 capping layer, ACS Appl. Mater. Interfaces **2**, 1565 (2010).

[76] J.-H. Cha and D.-Y. Jung, Air-stable transparent silver iodide–copper iodide heterojunction diode, ACS Appl. Mater. Interfaces **9**, 43807 (2017).

[77] A. Crovetto, H. Hempel, M. Rusu, L. Choubrac, D. Kojda, K. Habicht, and T. Unold, Water adsorption enhances electrical conductivity in transparent p-type CuI, ACS Appl. Mater. Interfaces **12**, 48741 (2020).

[78] A. K. Singh, L. Zhou, A. Shinde, S. K. Suram, J. H. Montoya, D. Winston, J. M. Gregoire, and K. A. Persson, Electrochemical stability of metastable materials, Chem. Mater. **29**, 10159 (2017).

[79] N. M. Twyman, A. Walsh, and T. Buonassisi, Environmental stability of crystals: A greedy screening, Chem. Mater. **34**, 2545 (2022).

[80] J. Willis, I. Bravić, R. R. Schnepf, K. N. Heinselman, B. Monserrat, T. Unold, A. Zakutayev, D. O. Scanlon, and A. Crovetto, Prediction and realisation of high mobility and degenerate p-type conductivity in CaCuP thin films, Chem. Sci. **13**, 5872 (2022).

[81] R. Cao, H.-X. Deng, and J.-W. Luo, Design principles of p-type transparent conductive materials, ACS Appl. Mater. Interfaces **11**, 24837 (2019).

[82] M. Chan and G. Ceder, Efficient band gap prediction for solids, Phys. Rev. Lett. **105**, 196403 (2010).

[83] M. Van Setten, M. Giantomassi, X. Gonze, G.-M. Rignanese, and G. Hautier, Automation methodologies and large-scale validation for *GW*: Towards high-throughput *GW* calculations, Phys. Rev. B **96**, 155207 (2017).

[84] C. Chen, Y. Zuo, W. Ye, X. Li, and S. P. Ong, Learning properties of ordered and disordered materials from multi-fidelity data, Nat. Comput. Sci. **1**, 46 (2021).

[85] Z. Yuan, D. Dahliah, M. R. Hasan, G. Kassa, A. Pike, S. Quadir, R. Claes, C. Chandler, Y. Xiong, V. Kyveryga, P. Yox, G.-M. Rignanese, I. Dabo, A. Zakutayev, D. P. Fenning, O. G. Reid, S. Bauers, J. Liu, K. Kovnir, and G. Hautier, Discovery of the Zintl-phosphide $BaCd_2P_2$ as a long carrier lifetime and stable solar absorber, Joule **8**, 1412 (2024).

[86] A. Walsh, J. L. Da Silva, S.-H. Wei, C. Körber, A. Klein, L. Piper, A. DeMasi, K. E. Smith, G. Panaccione, P. Torelli, D. J. Payne, A. Bourlange, and R. G. Egdell, Nature of the band gap of In_2O_3 revealed by first-principles calculations and x-ray spectroscopy, Phys. Rev. Lett. **100**, 167402 (2008).

[87] M. Baranowski, P. Plochocka, R. Su, L. Legrand, T. Barisien, F. Bernardot, Q. Xiong, C. Testelin, and M. Chamarro, Exciton binding energy and effective mass of $CsPbCl_3$: A magneto-optical study, Photonics Res. **8**, A50 (2020).

[88] J.-J. Zhou, J. Park, I.-T. Lu, I. Maliyov, X. Tong, and M. Bernardi, PERTURBO: A software package for *ab initio* electron-phonon interactions, charge transport and ultrafast dynamics, Comput. Phys. Commun. **264**, 107970 (2021).

[89] H. Lee, S. Poncé, K. Bushick, S. Hajinazar, J. Lafuente-Bartolome, J. Leveillee, C. Lian, J.-M. Lihm, F. Macheda, H. Mori, H. Paudyal, W. H. Sio, S. Tiwari, M. Zacharias, X. Zhang, N. Bonini, E. Kioupakis, E. R. M. Margine, and F. Giustino, Electron-phonon physics from first principles using the EPW code, npj Comput. Mater. **9**, 156 (2023).

[90] G. Brunin, H. P. C. Miranda, M. Giantomassi, M. Royo, M. Stengel, M. J. Verstraete, X. Gonze, G.-M. Rignanese, and G. Hautier, Phonon-limited electron mobility in Si, GaAs, and GaP with exact treatment of dynamical quadrupoles, Phys. Rev. B **102**, 094308 (2020).

[91] R. Claes, G. Brunin, M. Giantomassi, G.-M. Rignanese, and G. Hautier, Assessing the quality of relaxation-time approximations with fully automated computations of phonon-limited mobilities, Phys. Rev. B **106**, 094302 (2022).

[92] A. M. Ganose, J. Park, A. Faghaninia, R. Woods-Robinson, K. A. Persson, and A. Jain, Efficient calculation of carrier scattering rates from first principles, Nat. Commun. **12**, 2222 (2021).

[93] J. Willis, R. Claes, Q. Zhou, M. Giantomassi, G.-M. Rignanese, G. Hautier, and D. O. Scanlon, Limits to hole mobility and doping in copper iodide, Chem. Mater. **35**, 8995 (2023).

[94] D. Broberg, B. Medasani, N. E. Zimmermann, G. Yu, A. Canning, M. Haranczyk, M. Asta, and G. Hautier, PyCDT: A PYTHON toolkit for modeling point defects in semiconductors and insulators, Comput. Phys. Commun. **226**, 165 (2018).

[95] A. Goyal, P. Gorai, H. Peng, S. Lany, and V. Stevanović, A computational framework for automation of point defect calculations, Comput. Mater. Sci. **130**, 1 (2017).

[96] S. Hu, B. Xia, Y.-P. Lin, T. Katase, J. Fujioka, T. Kamiya, H. Hosono, K.-Z. Du, and Z. Xiao, p-type transparent quadruple perovskite halide conductors: Fact or fiction?, Adv. Funct. Mater. **30**, 1909906 (2020).

[97] J. Xu, J.-B. Liu, B.-X. Liu, and B. Huang, Exotic structural and optoelectronic properties of layered halide double perovskite polymorphs, Adv. Funct. Mater. **31**, 2008620 (2021).

[98] Y. Xiong, C. Bourgois, N. Sheremetyeva, W. Chen, D. Dahliah, H. Song, J. Zheng, S. M. Griffin, A. Sipahigil, and G. Hautier, High-throughput identification of spin-photon interfaces in silicon, Sci. Adv. **9**, 8617 (2023).

[99] J. C. Thomas, *et al.*, A substitutional quantum defect in WS_2 discovered by high-throughput computational screening and fabricated by site-selective STM manipulation, Nat. Commun. **15**, 3556 (2024).

[100] I. Mosquera-Lois, S. R. Kavanagh, A. Walsh, and D. O. Scanlon, Identifying the ground state structures of point defects in solids, npj Comput. Mater. **9**, 25 (2023).

[101] Y. Kumagai, Computational screening of p-type transparent conducting oxides using the optical absorption spectra and oxygen-vacancy formation energies, Phys. Rev. Appl. **19**, 034063 (2023).

[102] R. X. Yang, C. A. McCandler, O. Andriuc, M. Siron, R. Woods-Robinson, M. K. Horton, and K. A. Persson, Big data in a nano world: A review on computational, data-driven design of nanomaterials structures, properties, and synthesis, ACS Nano **16**, 19873 (2022).

[103] M. Morales-Masis, S. De Wolf, R. Woods-Robinson, J. W. Ager, and C. Ballif, Transparent electrodes for efficient optoelectronics, Adv. Electron. Mater. **3**, 1600529 (2017).

[104] D. Joshi and R. Srivastava, Mobility and carrier concentration in polycrystalline silicon, Solar Cells **12**, 337 (1984).

[105] K. Ellmer, D. Ginley, H. Hosono, and D. Paine, in *Transparent Conductive Zinc Oxide and Its Derivatives* (New York, 2010), p. 193.

[106] H. Marom, M. Ritterband, and M. Eizenberg, The contribution of grain boundary scattering versus surface scattering to the resistivity of thin polycrystalline films, Thin Solid Films **510**, 62 (2006).

[107] K. Ellmer and R. Mientus, Carrier transport in polycrystalline ITO and ZnO: Al II: The influence of grain barriers and boundaries, Thin Solid Films **516**, 5829 (2008).

[108] X. Wang, A. M. Ganose, S. R. Kavanagh, and A. Walsh, Band versus polaron: Charge transport in antimony chalcogenides, ACS Energy Lett. **7**, 2954 (2022).

[109] J.-H. Pöhls, S. Chanakian, J. Park, A. M. Ganose, A. Dunn, N. Friesen, A. Bhattacharya, B. Hogan, S. Bux, A. Jain, A. Mar, and A. Zevalkink, Experimental validation of high thermoelectric performance in $RECuZnP_2$ predicted by high-throughput DFT calculations, Mater. Horiz. **8**, 209 (2021).

[110] G. Jellison Jr, M. Chisholm, and S. Gorbatkin, Optical functions of chemical vapor deposited thin-film silicon determined by spectroscopic ellipsometry, Appl. Phys. Lett. **62**, 3348 (1993).

[111] N. Yamada, R. Ino, and Y. Ninomiya, Truly transparent p-type γ-CuI thin films with high hole mobility, Chem. Mater. **28**, 4971 (2016).

[112] L. Fanni, B. Aebersold, D. Alexander, L. Ding, M. M. Masis, S. Nicolay, and C. Ballif, c-texture versus a-texture low pressure metalorganic chemical vapor deposition ZnO films: Lower resistivity despite smaller grain size, Thin Solid Films **565**, 1 (2014).

[113] S. Kralj, P. Dally, P. Bampoulis, B. Vishal, S. De Wolf, and M. Morales-Masis, Impact of the TCO microstructure on the electronic properties of carbazole-based self-assembled monolayers, ACS Mater. Lett. **6**, 366 (2023).

[114] Y. Hu, J. Hwang, Y. Lee, P. Conlin, D. G. Schlom, S. Datta, and K. Cho, First principles calculations of intrinsic mobilities in tin-based oxide semiconductors SnO, SnO_2, and Ta_2SnO_6, J. Appl. Phys. **126**, 185701 (2019).

[115] A. R. Nagaraja, K. H. Stone, M. F. Toney, H. Peng, S. Lany, and T. O. Mason, Experimental characterization of a theoretically designed candidate p-type transparent conducting oxide: Li-doped Cr_2MnO_4, Chem. Mater. **26**, 4598 (2014).

[116] D. Dahliah, G.-M. Rignanese, and G. Hautier, Defect compensation in the p-type transparent oxide Ba_2BiTaO_6, J. Mater. Chem. C **8**, 9352 (2020).

[117] B. Ling, J. L. Zhao, X. W. Sun, S. T. Tan, A. K. K. Kyaw, Y. Divayana, and Z. L. Dong, Color tunable light-emitting diodes based on p^+-Si/p-$CuAlO_2$/n-ZnO nanorod array heterojunctions, Appl. Phys. Lett. **97**, 013101 (2010).

[118] R. Woods-Robinson, T. Ablekim, A. Norman, S. Johnston, K. A. Persson, M. O. Reese, W. K. Metzger, and A. Zakutayev, Sputtered p-type $Cu_xZn_{1-x}S$ back contact to CdTe solar cells, ACS Appl. Energy Mater. **3**, 5427 (2020).

[119] V. Raj, T. Lu, M. Lockrey, R. Liu, F. Kremer, L. Li, Y. Liu, H. H. Tan, and C. Jagadish, Introduction of TiO_2 in CuI for its improved performance as a p-type transparent conductor, ACS Appl. Mater. Interfaces **11**, 24254 (2019).

[120] R. Mehta and S. Vogel, Sputtered cadmium oxide and indium oxide/tin oxide films as transparent electrodes to cadmium sulfide, J. Electrochem. Soc. **119**, 752 (1972).

[121] I. Rauf, Structure and properties of tin-doped indium oxide thin films prepared by reactive electron-beam evaporation with a zone-confining arrangement, J. Appl. Phys. **79**, 4057 (1996).

[122] J. Robertson and Z. Zhang, Doping limits in p-type oxide semiconductors, MRS Bull. **46**, 1037 (2021).

[123] P. Storm, S. Gierth, S. Selle, M. Bar, H. von Wenckstern, M. Grundmann, and M. Lorenz, Evidence for oxygen being a dominant shallow acceptor in p-type CuI, APL Mater. **9**, 051101 (2021).

[124] K. R. Talley, J. Mangum, C. L. Perkins, R. Woods-Robinson, A. Mehta, B. P. Gorman, G. L. Brennecka, and A. Zakutayev, Synthesis of lanthanum tungsten oxynitride perovskite thin films, Adv. Electron. Mater. **5**, 1900214 (2019).

[125] F. V. E. Hensling, D. Dahliah, P. Dulal, P. Singleton, J. Sun, J. Schubert, H. Paik, I. Subedi, B. Subedi, G.-M. Rignanese, N. J. Podraza, G. Hautier, and D. G. Schlom, Epitaxial stannate pyrochlore thin films: Limitations of cation stoichiometry and electron doping, APL Mater. **9**, 051113 (2021).

[126] Y. Chen, S. Fan, and G. Gao, Design ambipolar conductivity on wide-gap semiconductors: The case of Al-and Na-doped CaS, Mater. Sci. Semicond. Process. **151**, 107024 (2022).

[127] G. Frank and H. Köstlin, Electrical properties and defect model of tin-doped indium oxide layers, Appl. Phys. A **27**, 197 (1982).
[128] A. Crovetto, T. S. Ottsen, E. Stamate, D. Kjær, J. Schou, and O. Hansen, On performance limitations and property correlations of Al-doped ZnO deposited by radio-frequency sputtering, J. Phys. D: Appl. Phys. **49**, 295101 (2016).
[129] R. Woods-Robinson, M. K. Horton, and K. A. Persson, A method to computationally screen for tunable properties of crystalline alloys, Patterns **4**, 100723 (2023).
[130] L. Chen, J. Yang, S. Klaus, L. J. Lee, R. Woods-Robinson, J. Ma, Y. Lum, J. K. Cooper, F. M. Toma, L.-W. Wang, I. D. Sharp, A. T. Bell, and J. W. Ager, p-type transparent conducting oxide/n-type semiconductor heterojunctions for efficient and stable solar water oxidation, J. Am. Chem. Soc. **137**, 9595 (2015).
[131] G. J. Exarhos, C. F. Windisch Jr, K. F. Ferris, and R. R. Owings, Cation defects and conductivity in transparent oxides, Appl. Phys. A **89**, 9 (2007).
[132] Y. Hu, D. Schlom, S. Datta, and K. Cho, Amorphous Ta_2SnO_6: A hole-dopable p-type oxide, Appl. Surf. Sci. **613**, 155981 (2023).
[133] L. A. Mittmann and A. Crovetto, Phosphosulfide semiconductors for optoelectronics and solar energy conversion, J. Phys.: Mater. **7**, 021002 (2024).
[134] P. J. McGinn, Thin-film processing routes for combinatorial materials investigations—a review, ACS Comb. Sci. **21**, 501 (2019).
[135] K. R. Talley, S. L. Millican, J. Mangum, S. Siol, C. B. Musgrave, B. Gorman, A. M. Holder, A. Zakutayev, and G. L. Brennecka, Implications of heterostructural alloying for enhanced piezoelectric performance of (Al,Sc)N, Phys. Rev. Mater. **2**, 063802 (2018).
[136] C. T. Parzyck, C. A. Pennington, W. J. I. DeBenedetti, J. Balajka, E. Echeverria, H. Paik, L. Moreschini, B. D. Faeth, C. Hu, J. K. Nangoi, V. Anil, T. A. Arias, M. A. Hines, D. G. Schlom, A. Galdi, K. M. Shen, and J. M. Maxson, Atomically smooth films of CsSb: A chemically robust visible light photocathode, APL Mater. **11**, 101125 (2023).
[137] R. R. Schnepf, A. Crovetto, P. Gorai, A. Park, M. Holtz, K. N. Heinselman, S. R. Bauers, M. Brooks Tellekamp, A. Zakutayev, A. L. Greenaway, E. S. Toberer, and A. C. Tamboli, Reactive phosphine combinatorial co-sputtering of cation disordered $ZnGeP_2$ films, J. Mater. Chem. C **10**, 870 (2022).
[138] D. P. Tabor, L. M. Roch, S. K. Saikin, C. Kreisbeck, D. Sheberla, J. H. Montoya, S. Dwaraknath, M. Aykol, C. Ortiz, H. Tribukait, C. Amador-Bedolla, C. J. Brabec, B. Maruyama, K. A. Persson, and A. Aspuru-Guzik, Accelerating the discovery of materials for clean energy in the era of smart automation, Nat. Rev. Mater. **3**, 5 (2018).
[139] S. Moradi, S. Kundu, and M. I. Saidaminov, High-throughput synthesis of thin films for the discovery of energy materials: A perspective, ACS Mater. Au **2**, 516 (2022).
[140] S. Fan and Y. Chen, The electronic structures and p-type performance of group IA and VA atoms in NiO: A first principles study, J. Appl. Phys. **131**, 135701 (2022).
[141] T. J. Jacobsson, *et al.*, An open-access database and analysis tool for perovskite solar cells based on the FAIR data principles, Nat. Energy **7**, 107 (2022).
[142] F. Hamelmann, J. Weicht, and G. Behrens, Light-induced degradation of thin film silicon solar cells, J. Phys.: Conf. Ser. **682**, 012002 (2016).
[143] M. Elnaggar, A. G. Boldyreva, M. Elshobaki, S. A. Tsarev, Y. S. Fedotov, O. R. Yamilova, S. I. Bredikhin, K. J. Stevenson, S. M. Aldoshin, and P. A. Troshin, Decoupling contributions of charge-transport interlayers to light-induced degradation of p-i-n perovskite solar cells, Solar RRL **4**, 2000191 (2020).
[144] G. K. Liyanage, A. B. Phillips, F. K. Alfadhili, R. J. Ellingson, and M. J. Heben, The role of back buffer layers and absorber properties for >25% efficient CdTe solar cells, ACS Appl. Energy Mater. **2**, 5419 (2019).
[145] A. Jafar, Ph.D. thesis, 2017.
[146] S. De Waele, K. Lejaeghere, M. Sluydts, and S. Cottenier, Error estimates for density-functional theory predictions of surface energy and work function, Phys. Rev. B **94**, 235418 (2016).
[147] K. T. Butler, G. Sai Gautam, and P. Canepa, Designing interfaces in energy materials applications with first-principles calculations, npj Comput. Mater. **5**, 19 (2019).
[148] B. A. Williamson, G. J. Limburn, G. W. Watson, G. Hyett, and D. O. Scanlon, Computationally driven discovery of layered quinary oxychalcogenides: Potential p-type transparent conductors?, Matter **3**, 759 (2020).
[149] P. M. Salome, B. Vermang, R. Ribeiro-Andrade, J. P. Teixeira, J. M. Cunha, M. J. Mendes, S. Haque, J. Borme, H. Aguas, E. Fortunato, R. Martins, J. C. González, J. P. Leitão, P. A. Fernandes, M. Edoff, and S. Sadewasser, Passivation of interfaces in thin film solar cells: Understanding the effects of a nanostructured rear point contact layer, Adv. Mater. Interfaces **5**, 1701101 (2018).
[150] E. Aydin, M. De Bastiani, and S. De Wolf, Defect and contact passivation for perovskite solar cells, Adv. Mater. **31**, 1900428 (2019).
[151] M. D. Jones, J. A. Dawson, S. Campbell, V. Barrioz, L. D. Whalley, and Y. Qu, Modelling interfaces in thin-film photovoltaic devices, Front. Chem. **10**, 920676 (2022).
[152] B. Yang, D. Ouyang, Z. Huang, X. Ren, H. Zhang, and W. C. Choy, Multifunctional synthesis approach of In:$CuCrO_2$ nanoparticles for hole transport layer in high-performance perovskite solar cells, Adv. Funct. Mater. **29**, 1902600 (2019).
[153] Y. Smirnov, L. Schmengler, R. Kuik, P.-A. Repecaud, M. Najafi, D. Zhang, M. Theelen, E. Aydin, S. Veenstra, S. De Wolf, and M. Morales Masis, Scalable pulsed laser deposition of transparent rear electrode for perovskite solar cells, Adv. Mater. Technol. **6**, 2000856 (2021).
[154] W. Soltanpoor, A. E. Bracesco, N. Rodkey, M. Creatore, and M. Morales-Masis, Low damage scalable pulsed laser deposition of SnO_2 for p-i-n perovskite solar cells, Solar RRL **7**, 2300616 (2023).
[155] T. D. Lee and A. U. Ebong, A review of thin film solar cell technologies and challenges, Renewable Sustainable Energy Rev. **70**, 1286 (2017).
[156] S. Abbott, Practical coatings: Pinholes, https://www.stevenabbott.co.uk/practical-coatings/pinholes.php, 2023 (Accessed on: 2023-12-14).

[157] Y. Smirnov, P.-A. Repecaud, L. Tutsch, I. Florea, K. P. Zanoni, A. Paliwal, H. J. Bolink, P. R. I. Cabarrocas, M. Bivour, and M. Morales-Masis, Wafer-scale pulsed laser deposition of ITO for solar cells: Reduced damage vs. interfacial resistance, Mater. Adv. **3**, 3469 (2022).

[158] K. P. Zanoni, A. Paliwal, M. A. Hernández-Fenollosa, P.-A. Repecaud, M. Morales-Masis, and H. J. Bolink, Ito top-electrodes via industrial-scale PLD for efficient buffer-layer-free semitransparent perovskite solar cells, Adv. Mater. Technol. **7**, 2101747 (2022).

[159] M. Roffeis, S. Kirner, J.-C. Goldschmidt, B. Stannowski, L. M. Perez, C. Case, and M. Finkbeiner, New insights into the environmental performance of perovskite-on-silicon tandem solar cells—A life cycle assessment of industrially manufactured modules, Sustainable Energy Fuels **6**, 2924 (2022).

[160] M. A. Scarpulla, *et al.*, CdTe-based thin film photovoltaics: Recent advances, current challenges and future prospects, Sol. Energy Mater. Sol. Cells **255**, 112289 (2023).

[161] G. Li, Y. Jiang, S. Deng, A. Tam, P. Xu, M. Wong, and H.-S. Kwok, Overcoming the limitations of sputtered nickel oxide for high-efficiency and large-area perovskite solar cells, Adv. Sci. **4**, 1700463 (2017).

[162] A. Liu, H. Zhu, M.-G. Kim, J. Kim, and Y.-Y. Noh, Engineering copper iodide (CuI) for multifunctional *p*-type transparent semiconductors and conductors, Adv. Sci. **8**, 2100546 (2021).

[163] L. A. Zafoschnig, S. Nold, and J. C. Goldschmidt, The race for lowest costs of electricity production: Techno-economic analysis of silicon, perovskite and tandem solar cells, IEEE J. Photovoltaics **10**, 1632 (2020).

[164] P. Gorai, D. Krasikov, S. Grover, G. Xiong, W. K. Metzger, and V. Stevanović, A search for new back contacts for CdTe solar cells, Sci. Adv. **9**, eade3761 (2023).

[165] C. Perkins, Collaborative R&D with First Solar on understanding performance limitations in CdTe, Cooperative Research and Development Final Report CRD-13-00507 [National Renewable Energy Laboratory (NREL), Golden, Colorado, 2023].

[166] R. Owen, J. Stilgoe, P. Macnaghten, M. Gorman, E. Fisher, and D. Guston, in *Responsible Innovation: Managing the Responsible Emergence of Science and Innovation in Society* (Wiley, Chichester, West Sussex, 2013), p. 27.

[167] B. A. Wender, R. W. Foley, T. A. Hottle, J. Sadowski, V. Prado-Lopez, D. A. Eisenberg, L. Laurin, and T. P. Seager, Anticipatory life-cycle assessment for responsible research and innovation, J. Responsible Innov. **1**, 200 (2014).

[168] D. W. Pennington, J. Potting, G. Finnveden, E. Lindeijer, O. Jolliet, T. Rydberg, and G. Rebitzer, Life cycle assessment part 2: Current impact assessment practice, Environ. Int. **30**, 721 (2004).

[169] NREL, Life cycle greenhouse gas emissions from electricity generation: Update, Tech. Rep., National Renewable Energy Laboratory (NREL), Golden, Colorado, 2021.

[170] J. D. Bergesen, G. A. Heath, T. Gibon, and S. Suh, Thin-film photovoltaic power generation offers decreasing greenhouse gas emissions and increasing environmental co-benefits in the long term, Environ. Sci. Technol. **48**, 9834 (2014).

[171] Energy Technology Perspectives 2023, Tech. Rep., International Energy Agency (IEA), 2023.

[172] V. Fthenakis, Sustainability of photovoltaics: The case for thin-film solar cells, Renewable Sustainable Energy Rev. **13**, 2746 (2009).

[173] A. Rashedi and T. Khanam, Life cycle assessment of most widely adopted solar photovoltaic energy technologies by mid-point and end-point indicators of ReCiPe method, Environ. Sci. Pollut. Res. **27**, 29075 (2020).

[174] S. Lee and A. Manthiram, Can cobalt be eliminated from lithium-ion batteries?, ACS Energy Lett. **7**, 3058 (2022).

[175] S. Husein, R. Woods-Robinson, and R. Saive, in *2021 IEEE 48th Photovoltaic Specialists Conference (PVSC)* (IEEE, Fort Lauderdale, FL, USA, 2021).

[176] V. L. Putsche, J. Pattany, T. Ghosh, S. Atnoorkar, J. Zuboy, A. Carpenter, E. S. Takeuchi, A. C. Marschilok, K. J. Takeuchi, A. Burrell, and M. K. Mann, A framework for integrating supply chain, environmental, and social justice factors during early stationary battery research, Front. Sustain. **4**, 1287423 (2023).

[177] W. Ke and M. G. Kanatzidis, Prospects for low-toxicity lead-free perovskite solar cells, Nat. Commun. **10**, 965 (2019).

[178] M. D. Horgan, H. A. Hsain, J. L. Jones, and K. D. Grieger, Development and application of screening-level risk analysis for emerging materials, Sustain. Mater. Technol. **35**, e00524 (2023).

[179] S. Weyand, K. Kawajiri, C. Mortan, and L. Schebek, Scheme for generating upscaling scenarios of emerging functional materials based energy technologies in prospective LCA (UpFunMatLCA), J. Ind. Ecol. **27**, 676 (2023).

[180] B. A. Wender, R. W. Foley, V. Prado-Lopez, D. Ravikumar, D. A. Eisenberg, T. A. Hottle, J. Sadowski, W. P. Flanagan, A. Fisher, L. Laurin, M. E. Bates, I. Linkov, T. P. Seager, M. P. Fraser, and D. H. Guston, Illustrating anticipatory life cycle assessment for emerging photovoltaic technologies, Environ. Sci. Technol. **48**, 10531 (2014).

[181] C. Mutel, BRIGHTWAY: An open source framework for life cycle assessment, J. Open Source Softw. **2**, 236 (2017).